

Hydro-Elastic Analysis of Marine Structures Using a Boundary Integral Equation Method

L. Kaydıhan², B. Uğurlu¹ and A. Ergin¹

¹ Faculty of Naval Architecture and Ocean Eng., ITU,
Turkey

² Delta Marine, Turkey

Hydroelasticity Research Group in ITU

Professor A. Ergin, ITU

Dr. B. Uğurlu, ITU

L. Kaydıhan, DELTA MARINE TURKEY

S.A. Köroğlu, ITU

Activities of Research Group

- General 3D Hydroelasticity Method
- Experimental studies; modal analysis, operational modal analysis, vibration measurements
- Outcomes are reported in *Journal of Sound and Vibration* and *Journal of Fluids and Structures*
- Research Projects founded by *Technical Research Council of Turkey*

MATHEMATICAL MODEL

Fluid – Structure Interaction Problem

The fluid is assumed ideal, i.e., inviscid and incompressible, and its motion is irrotational and there exists a fluid velocity vector, \mathbf{v} , which can be defined as the gradient of the velocity potential function Φ as

$$\mathbf{v}(x, y, z, t) = \nabla \Phi(x, y, z, t) \quad (1)$$

The velocity potential Φ may be expressed as

$$\Phi = U x + \phi \quad (2)$$

MATHEMATICAL MODEL

Fluid – Structure Interaction Problem

Here the steady velocity potential U represents the effect of the mean flow associated with the undisturbed flow velocity U in the Axial direction. Further, ϕ is the unsteady velocity potential associated with the perturbations to the flow field due to the motion of the flexible body and satisfies the Laplace equation

$$\nabla^2 \phi = 0 \quad (3)$$

throughout the fluid domain. For the structure immersed in and/or containing flowing fluid, the vibratory response of the structure may be expressed in terms of principal coordinates as

$$\mathbf{p}(t) = \mathbf{p}_0 e^{\lambda t} \quad (4)$$

MATHEMATICAL MODEL

Fluid – Structure Interaction Problem

The velocity potential function due to the distortion of the structure in the *r*th *in vacuo* vibrational mode may be written as follows

$$\phi_r(x, y, z, t) = \phi_r(x, y, z) p_{0r} e^{\lambda t} \quad (5)$$

where M represents the number of modes of interest, and p_{0r} is an unknown complex amplitude for the *r*th principal coordinate.

On the wetted surface of the vibrating structure the normal fluid velocity must equal to the normal velocity on the structure and this condition for the *r*th modal vibration of the elastic structure containing and/or submerged in flowing fluid can be expressed as

$$\frac{\partial \phi_r}{\partial n} = \left(\frac{\partial \mathbf{u}_r}{\partial t} + U \frac{\partial \mathbf{u}_r}{\partial x} \right) \cdot \mathbf{n} \quad (6)$$

MATHEMATICAL MODEL

Fluid – Structure Interaction Problem

The vector \mathbf{u}_r denotes the displacement response of the structure in the r th principal coordinate and it may be written as

$$\mathbf{u}_r(x, y, z, t) = \mathbf{u}_r(x, y, z) p_{0r} e^{\lambda t} \quad (7)$$

Substituting Eqs. (5) and (7) into (6), the following expression is obtained for the boundary condition on the fluid-structure interface

$$\frac{\partial \phi_r}{\partial \mathbf{n}} = \lambda \mathbf{u}_r(x, y, z) \cdot \mathbf{n} + U \frac{\partial \mathbf{u}_r(x, y, z)}{\partial x} \cdot \mathbf{n} \quad (8)$$

MATHEMATICAL MODEL

Fluid – Structure Interaction Problem

It is assumed that the elastic structure vibrates at relatively high frequencies so that the effect of surface waves can be neglected. Therefore, the free surface condition (infinite frequency limit condition) for the perturbation potential can be approximated by

$$\phi_r = 0 \quad \text{on the free surface} \quad (9)$$

The method of images may be used to satisfy this boundary condition. By adding an imaginary boundary region, the condition given by Eq. (9) at the horizontal surface can be omitted; thus the problem is reduced to a classical Neumann case. It should be noted that, for the completely filled elastic structure, the normal fluid velocity cannot be arbitrarily specified. It has to satisfy the incompressibility condition

$$\iint_{S_w + S_{im}} \frac{\partial \phi_r}{\partial \mathbf{n}} dS = 0, \quad (10)$$

MATHEMATICAL MODEL

Numerical Evaluation of Perturbation Potential

The boundary value problem for the perturbation potential, may be expressed in the following form:

$$c(\xi)\phi(\xi) = \iint_{S_w} (\phi^*(s, \xi)q(s) - \phi(s)q^*(s, \xi)) dS \quad (11)$$

where ξ and s denote, respectively, the evaluation and field points on the wetted surface. ϕ^* is the fundamental solution and expressed as follows,

$$\phi^*(s, \xi) = \frac{1}{4\pi r} \quad (12)$$

MATHEMATICAL MODEL

Numerical Evaluation of Perturbation Potential

$q = \partial \phi / \partial \mathbf{n}$ is the flux, and r the distance between the evaluation and field points. The free term is defined as the fraction of that lies inside the domain of interest. Moreover, $q^*(s, \xi)$ can be written as

$$q^*(s, \xi) = -(\partial r / \partial \mathbf{n}) / 4 \pi r^3 \quad (13)$$

The fluid-structure interaction problem may be separated into two parts: (i) the vibration of the elastic structure in a quiescent fluid, and (ii) the disturbance in the main axial flow due to the oscillation of the structure. Thus, defining ϕ , Eq (7) may be divided into two separate parts as

$$\frac{\partial \phi_1}{\partial \mathbf{n}} = \mathbf{u}(x, y, z) \cdot \mathbf{n}, \quad \frac{\partial \phi_2}{\partial \mathbf{n}} = \frac{\partial \mathbf{u}(x, y, z)}{\partial x} \cdot \mathbf{n}, \quad (14a,b)$$

MATHEMATICAL MODEL

Numerical Evaluation of Perturbation Potential

For the solution of Eq. (11) with boundary conditions (14a and b), the wetted surface can be idealized by using boundary elements, referred to as hydrodynamic panels, and the distribution of the potential function and its flux over each hydrodynamic panel may be described in terms of the shape functions and nodal values as

$$\phi_e = \sum_{j=1}^{n_e} N_{ej} \phi_{ej}, \quad q_e = \sum_{j=1}^{n_e} N_{ej} q_{ej} \quad (15)$$

Here, n_e represents the number of nodal points assigned to each hydrodynamic panel, and N_{ej} the shape function adopted for the distribution of the potential function. e and j indicates the numbers of the hydrodynamic panels and nodal points, respectively.

MATHEMATICAL MODEL

Numerical Evaluation of Perturbation Potential

In the case of a linear distribution adopted in this study, the shape functions for a quadrilateral panel may be expressed as

$$N_{e1} = ((1-\zeta)(1-\eta))/4$$

$$N_{e2} = ((1+\zeta)(1-\eta))/4$$

$$N_{e3} = ((1+\zeta)(1+\eta))/4$$

$$N_{e4} = ((1-\zeta)(1+\eta))/4$$

(16)

MATHEMATICAL MODEL

Numerical Evaluation of Perturbation Potential

After substituting Eqs. (15) and (16) into Eq. (11) and applying the boundary conditions given in Eqs. (14a) and (14b), the unknown potential function values can be determined from the following sets of algebraic equations

$$c_k \phi_{1k} + \sum_{i=1}^m \sum_{j=1}^{n_m} (\phi_{1ij} \iint_{\Delta S_i} N_j q^* dS = \sum_{i=1}^m \sum_{j=1}^{n_m} (\mathbf{u}_{ij} \cdot \mathbf{n}_j \iint_{\Delta S_i} N_j \phi^* dS), \quad (17 \text{ a})$$

$$c_k \phi_{2k} + \sum_{i=1}^m \sum_{j=1}^{n_m} (\phi_{2ij} \iint_{\Delta S_i} N_j q^* dS = \sum_{i=1}^m \sum_{j=1}^{n_m} \left(\frac{\partial \mathbf{u}_{ij}}{\partial x} \cdot \mathbf{n}_j \iint_{\Delta S_i} N_j \phi^* dS \right),$$

$$k = 1, 2, \dots, m$$

where m denotes the number of nodal points used in the discretization of the structure

MATHEMATICAL MODEL

Calculation of Generalized Fluid-Structure

Interaction Force Coefficients

Using the Bernoulli's equation and neglecting the second order terms, the dynamic fluid pressure on the elastic structure due to the r th modal vibration becomes

$$P_r(x, y, z, t) = -\rho \left(\frac{\partial \phi_r}{\partial t} + U \frac{\partial \phi_r}{\partial x} \right), \quad (18)$$

Substituting equation (5) into (18), the following expression for the pressure is obtained,

$$P_r(x, y, z, t) = -\rho \left(\lambda \phi_r + U \frac{\partial \phi_r}{\partial x} \right) p_{0r} e^{\lambda t}. \quad (19)$$

MATHEMATICAL MODEL

Calculation of Generalized Fluid-Structure Interaction Force Coefficients

By using the definition of $\phi_r = \lambda \phi_{r1} + U \phi_{r2}$, equation (19) may be rewritten in the following form:

$$P_r(x, y, z, t) = -\rho \left(\lambda^2 \phi_{r1} + U \lambda \left(\frac{\partial \phi_{r1}}{\partial x} + \phi_{r2} \right) + U^2 \frac{\partial \phi_{r2}}{\partial x} \right) p_{0r} e^{\lambda t} \quad (20)$$

The *kth* component of the generalized fluid-structure interaction force due to the *rth* modal *in-vacuo* vibration of the elastic structure subjected to axial flow can be expressed in terms of the pressure acting on the wetted surface of the structure as

MATHEMATICAL MODEL

Calculation of Generalized Fluid-Structure Interaction Force Coefficients

$$\begin{aligned} Z_{kr} &= \iint_{S_w} P_r(x, y, z, t) \mathbf{u}_k \mathbf{n} dS \\ &= -p_{0r} e^{\lambda t} \iint_{S_w} \rho \left(\lambda^2 \phi_{r1} + U \lambda \left(\frac{\partial \phi_{r1}}{\partial x} + \phi_{r2} \right) + U^2 \frac{\partial \phi_{r2}}{\partial x} \right) \mathbf{u}_k \mathbf{n} dS \\ &= -\lambda^2 p_{0r} e^{\lambda t} \rho \iint_{S_w} \phi_{r1} \mathbf{u}_k \mathbf{n} dS - \lambda p_{0r} e^{\lambda t} \rho U \iint_{S_w} \left(\frac{\partial \phi_{r1}}{\partial x} + \phi_{r2} \right) \mathbf{u}_k \mathbf{n} dS \\ &\quad - p_{0r} e^{\lambda t} \rho U^2 \iint_{S_w} \frac{\partial \phi_{r2}}{\partial x} \mathbf{u}_k \mathbf{n} dS \end{aligned} \tag{21}$$

MATHEMATICAL MODEL

Calculation of Generalized Fluid-Structure Interaction Force Coefficients

The generalized added mass, A_{kr} , generalized fluid damping (due to the Coriolis effect of fluid), B_{kr} and generalized fluid stiffness (due to the centrifugal effect of fluid), C_{kr} terms can be defined as

$$A_{kr} = \rho \iint_{S_w} \phi_{r1} \mathbf{u}_k \mathbf{n} dS, \quad (22)$$

$$B_{kr} = \rho U \iint_{S_w} \left(\frac{\partial \phi_{r1}}{\partial x} + \phi_{r2} \right) \mathbf{u}_k \mathbf{n} dS, \quad (23)$$

$$C_{kr} = \rho U^2 \iint_{S_w} \frac{\partial \phi_{r2}}{\partial x} \mathbf{u}_k \mathbf{n} dS. \quad (24)$$

MATHEMATICAL MODEL

Calculation of Generalized Fluid-Structure Interaction Force Coefficients

Therefore, the generalized fluid-structure interaction force component, Z_{kr} , can be written as

$$\begin{aligned} Z_{kr}(t) &= -A_{kr} \lambda^2 p_{0r} e^{\lambda t} - B_{kr} \lambda p_{0r} e^{\lambda t} - C_{kr} p_{0r} e^{\lambda t} \\ &= -A_{kr} \ddot{p}_r(t) - B_{kr} \dot{p}_r(t) - C_{kr} p_r(t) \end{aligned} \quad (25)$$

MATHEMATICAL MODEL

Calculation of Wet Frequencies and Mode Shapes

The generalized equation of motion for the elastic structure in contact with axial flow assuming free vibrations with no structural damping is

$$\left[\lambda^2 (\mathbf{a} + \mathbf{A}) + \lambda (\mathbf{B}) + (\mathbf{c} + \mathbf{C}) \right] \mathbf{p} = 0, \quad (26)$$

where \mathbf{a} and \mathbf{c} denote the generalized structural mass and stiffness matrices, respectively, and they are calculated by using a standard finite element program [21]. The matrices \mathbf{A} , \mathbf{B} and \mathbf{C} represent the generalized added mass, generalized fluid damping and generalized fluid stiffness matrices, respectively.

Hydroelastic Investigation of a 1900 TEU Container Ship

MAIN PARTICULARS

Length overall	:	182.85 m
Length perpendicular	:	171.00 m
Breadth (moulded)	:	28.00 m
Depth (moulded)	:	16.10 m
Design draught	:	10.00 m
Scantling draught	:	11.00 m
Service speed	:	19.50 knot
Deadweight (at scantling draught)	:	26200 ton

1900 TEU CONTAINER SHIP

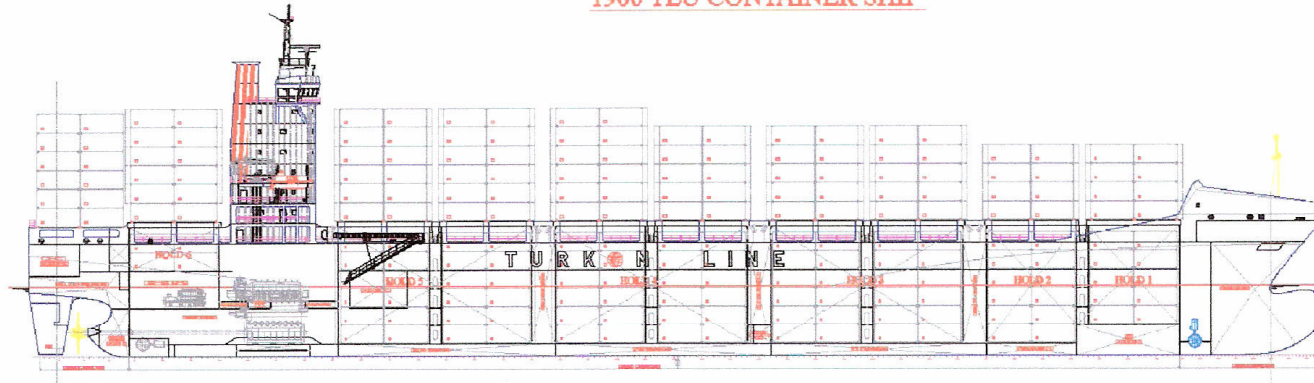


Figure 1 – General arrangement

Hydroelastic Investigation of a 1900 TEU Container Ship – FE Model

- FE calculations were carried out by Delta Marine, Turkey.
- Abaqus employed for the FE calculations
- Ship Model is developed in two parts;
Aft part consists of engine room, poop deck, aft peak and Superstructure decks.
Fore part consists of cargo area, fore peak, forecastle deck
- Fine mesh density is used for the aft part model

Hydroelastic Investigation of a 1900 TEU Container Ship – FE Model

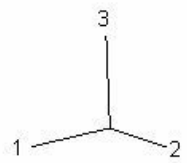
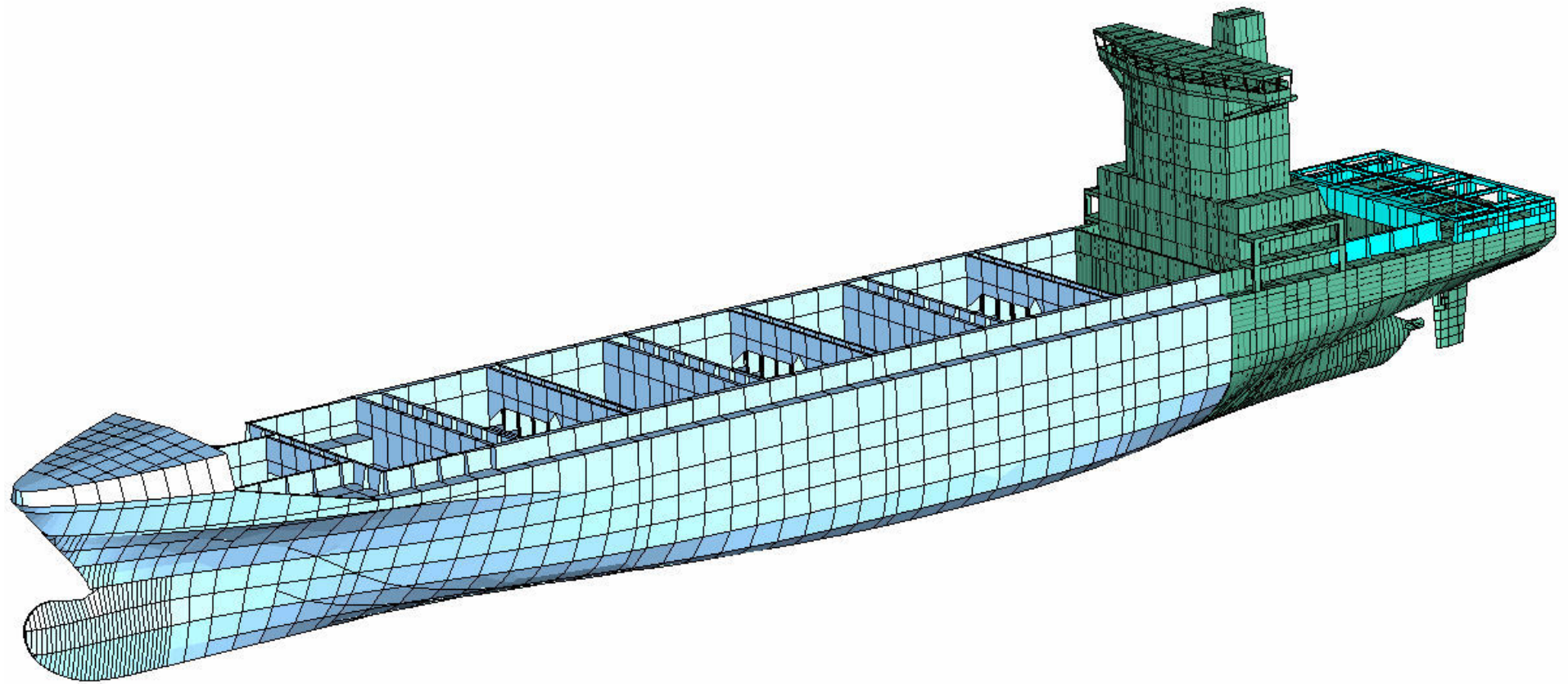
- Cargo loading is applied as inertia mass elements distributed over the cargo area inner bottom plating
- Ballast weights, heavy fuel oil and other tank weights are also applied as inertial mass elements.
- Finite elements model has 176030 nodes, 176800 structural elements

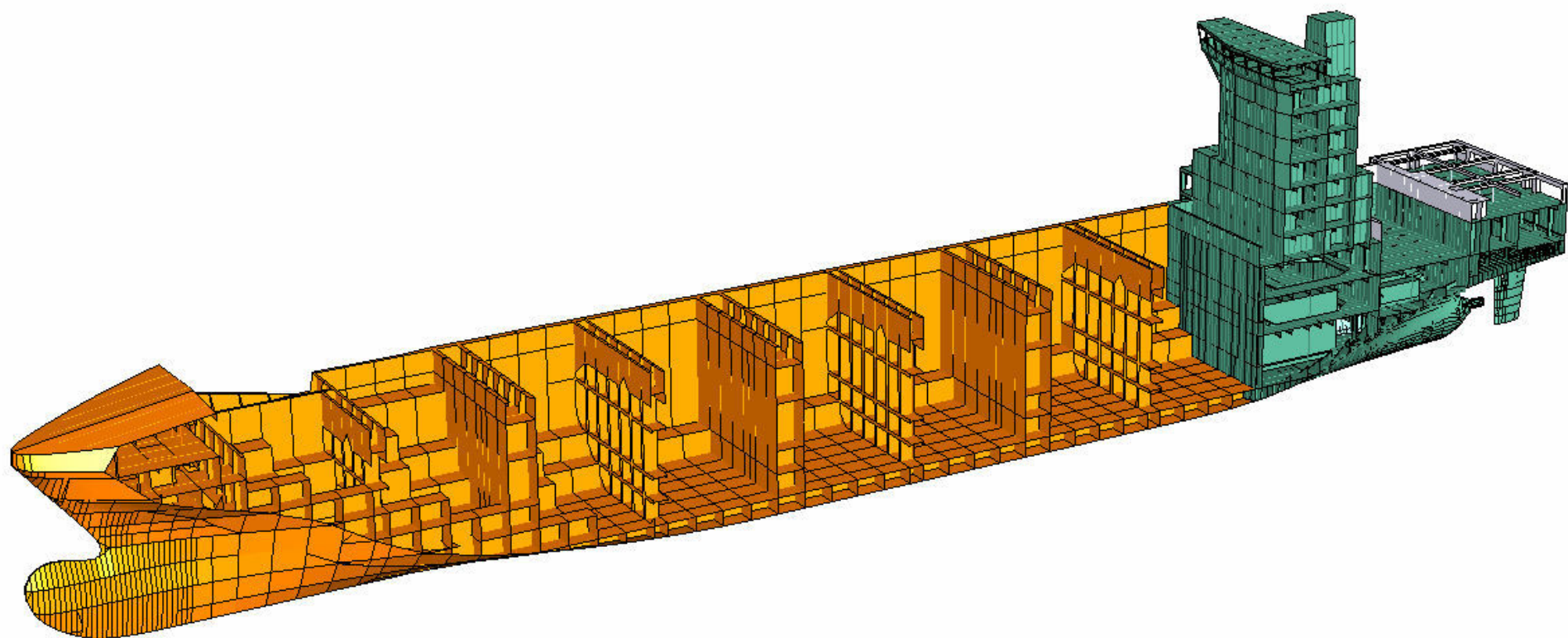
Hydroelastic Investigation of a 1900 TEU Container Ship – FE Model – Loading Cond.

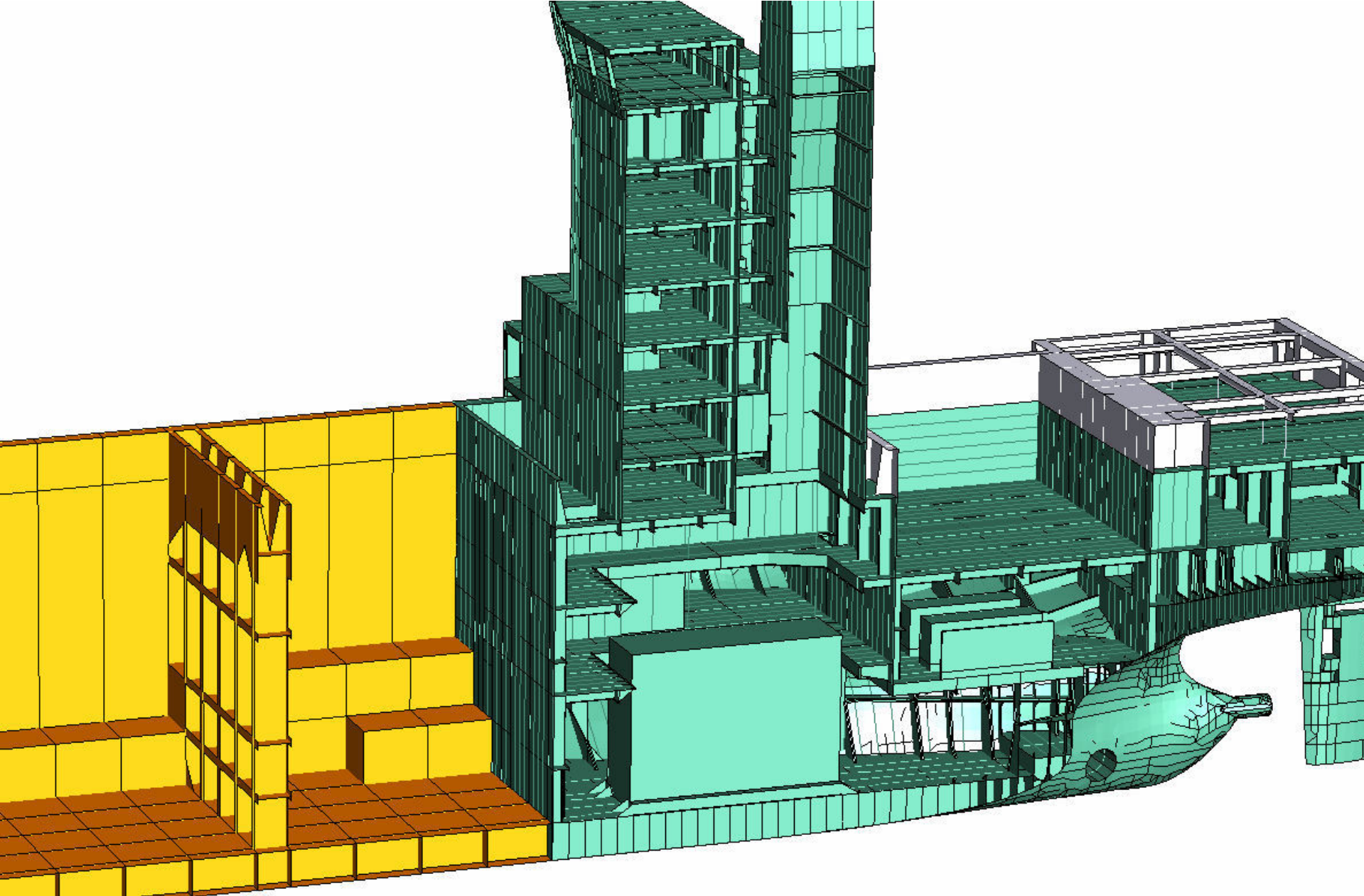
- Full loading with design draught of 10 m.
- Cargo loading – 17150 t
- Ballast weight – 3021 t
- Heavy fuel oil – 1886 t
- Marine diesel oil – 165 t
- Fresh water – 206 t
- Other tank weights – 165 t

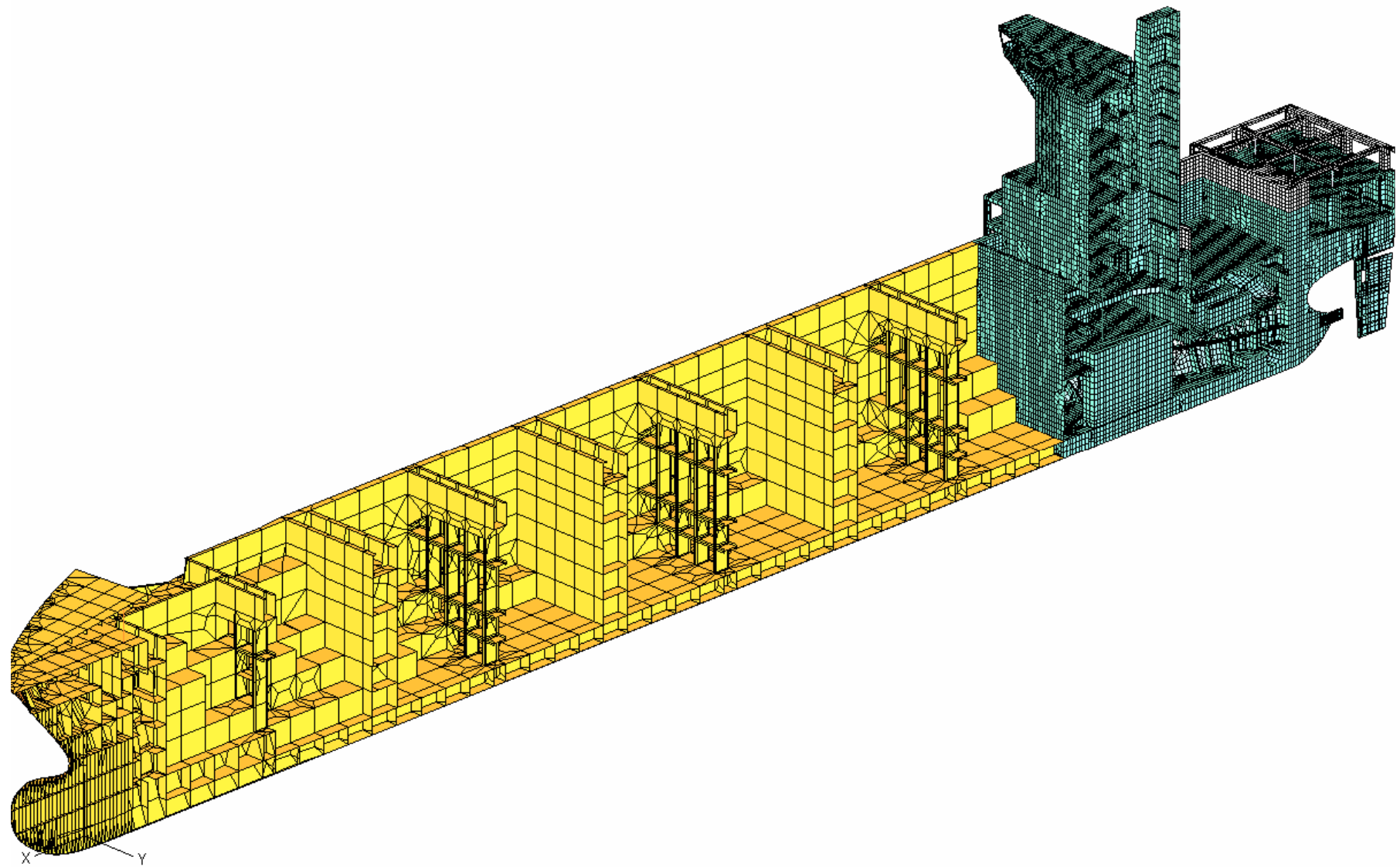
Hydroelastic Investigation of a 1900 TEU Container Ship – FE Model – Loading Cond.

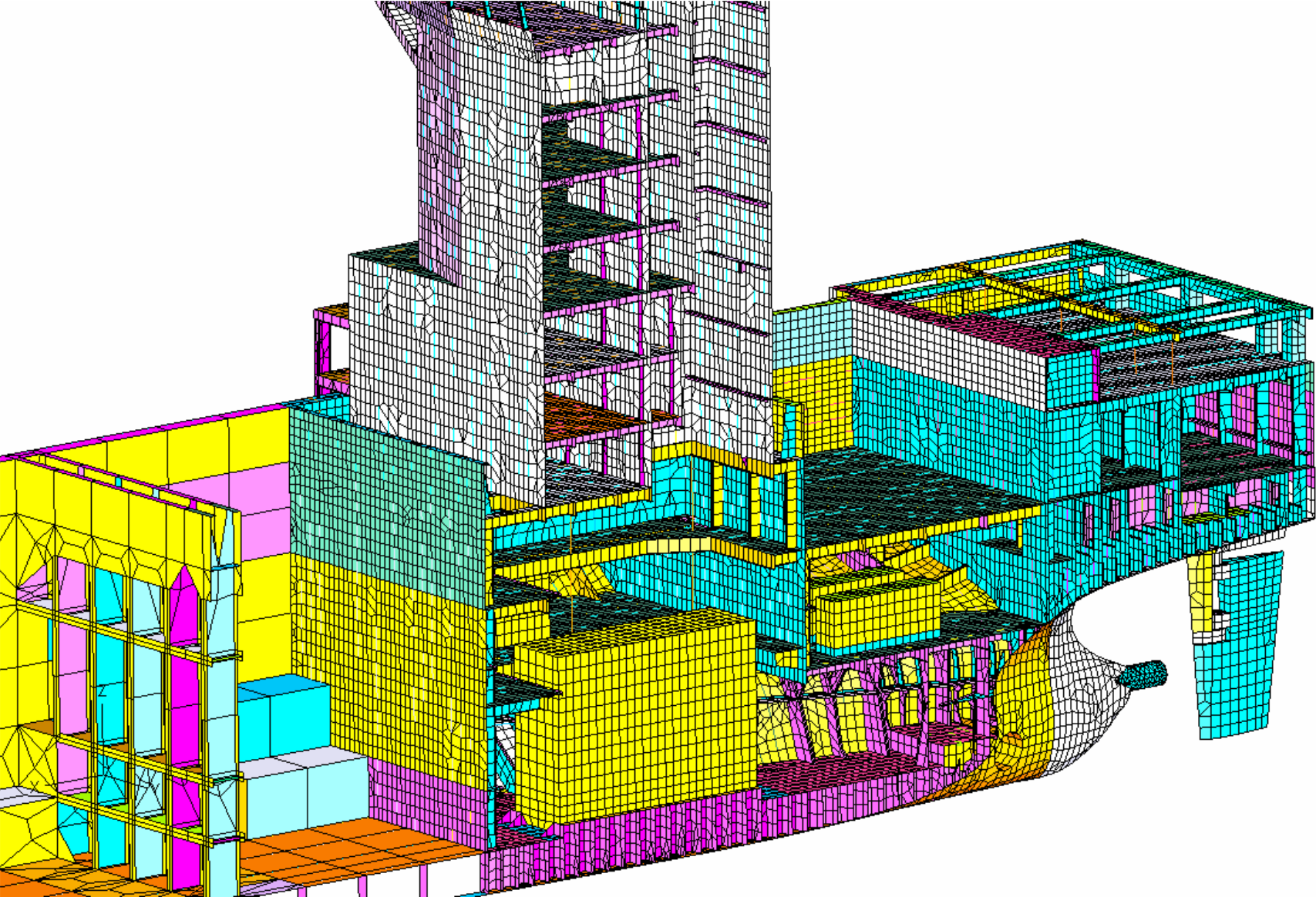
- LWT – 9000 t
- DWT – 22595.7 t
- Total Weight – 31595.7 t
- Total Finite Element Weight – 31520 t
- LCG – 79.85 m
- LCG – FEM – 80.3 m



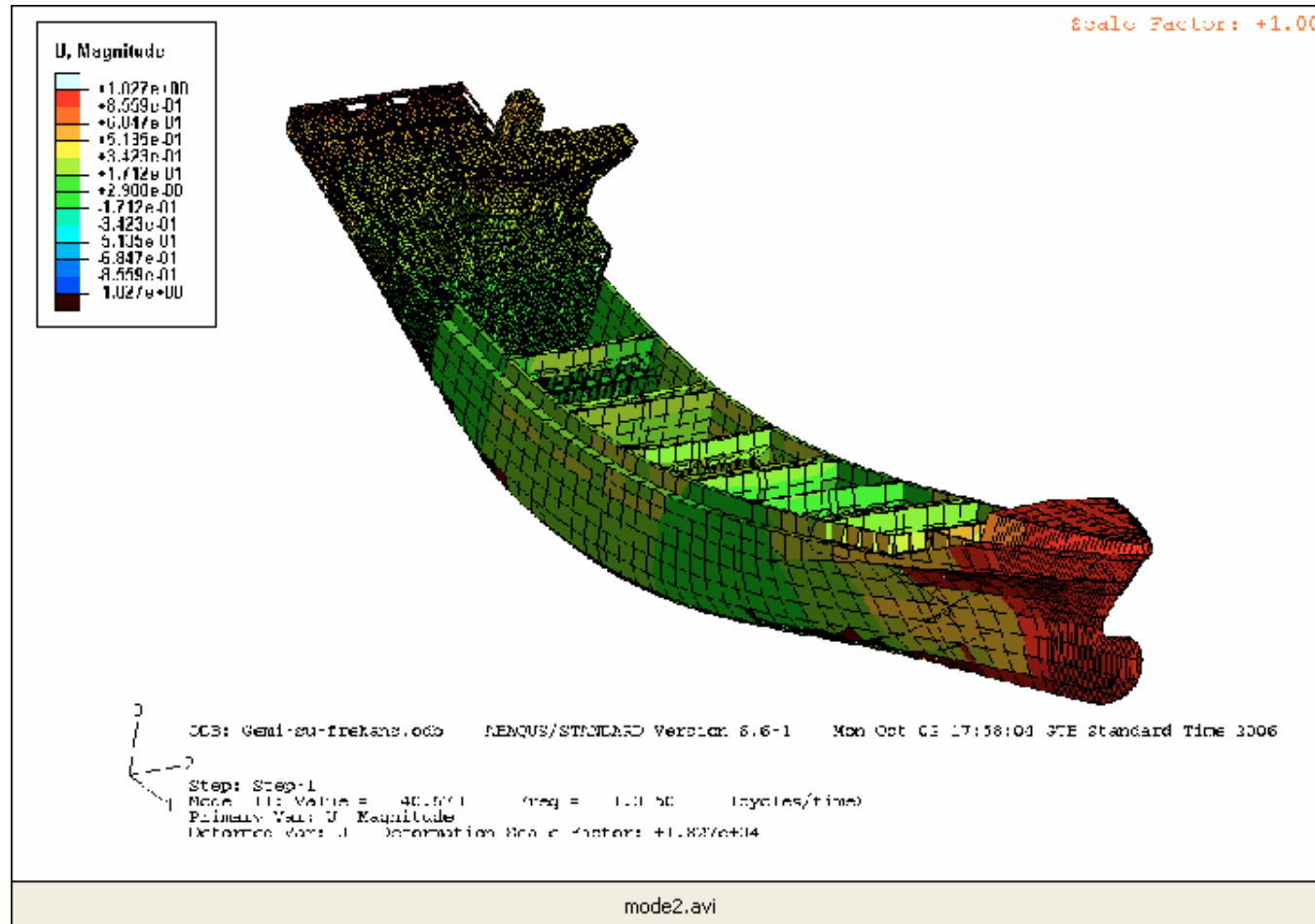




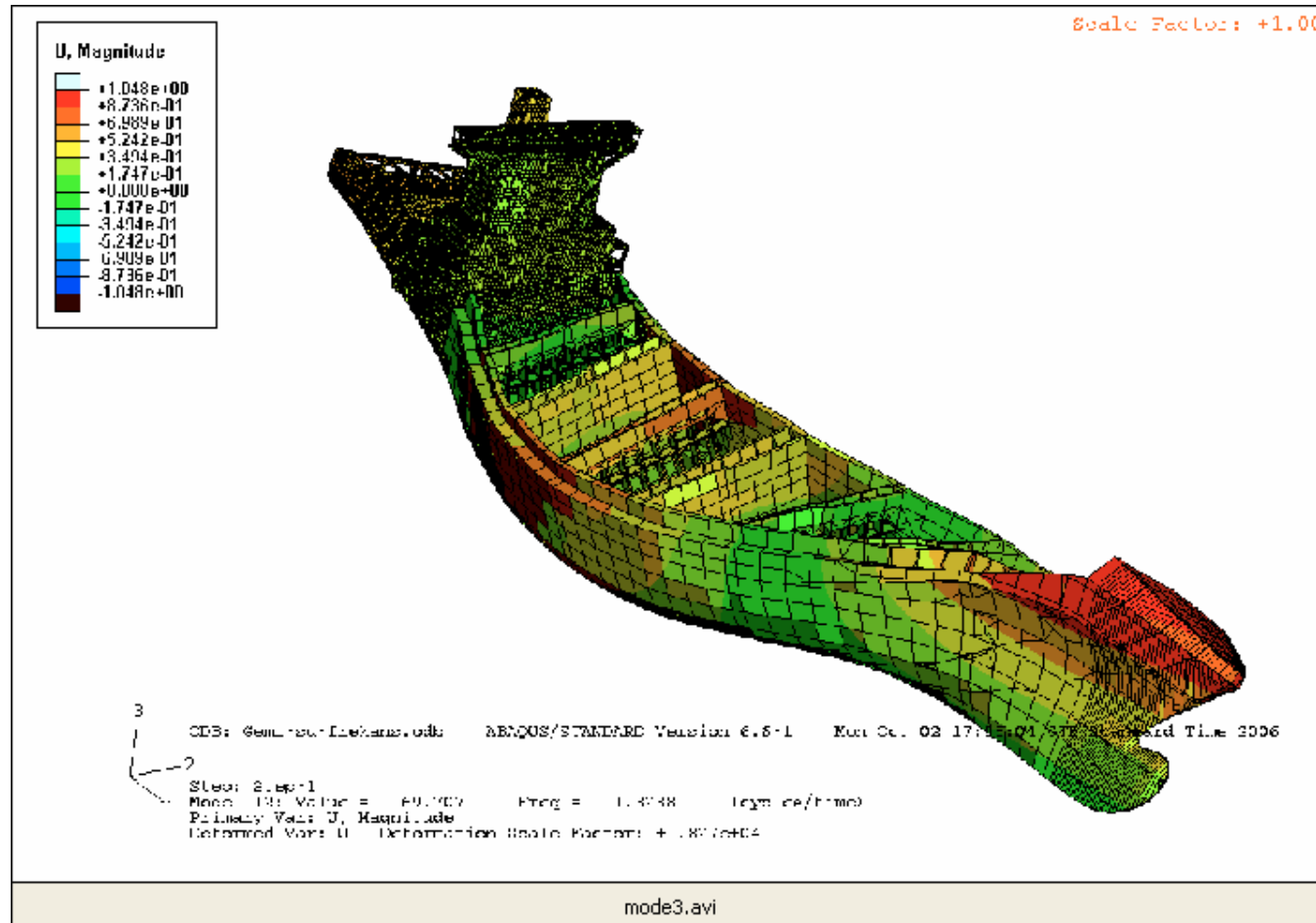




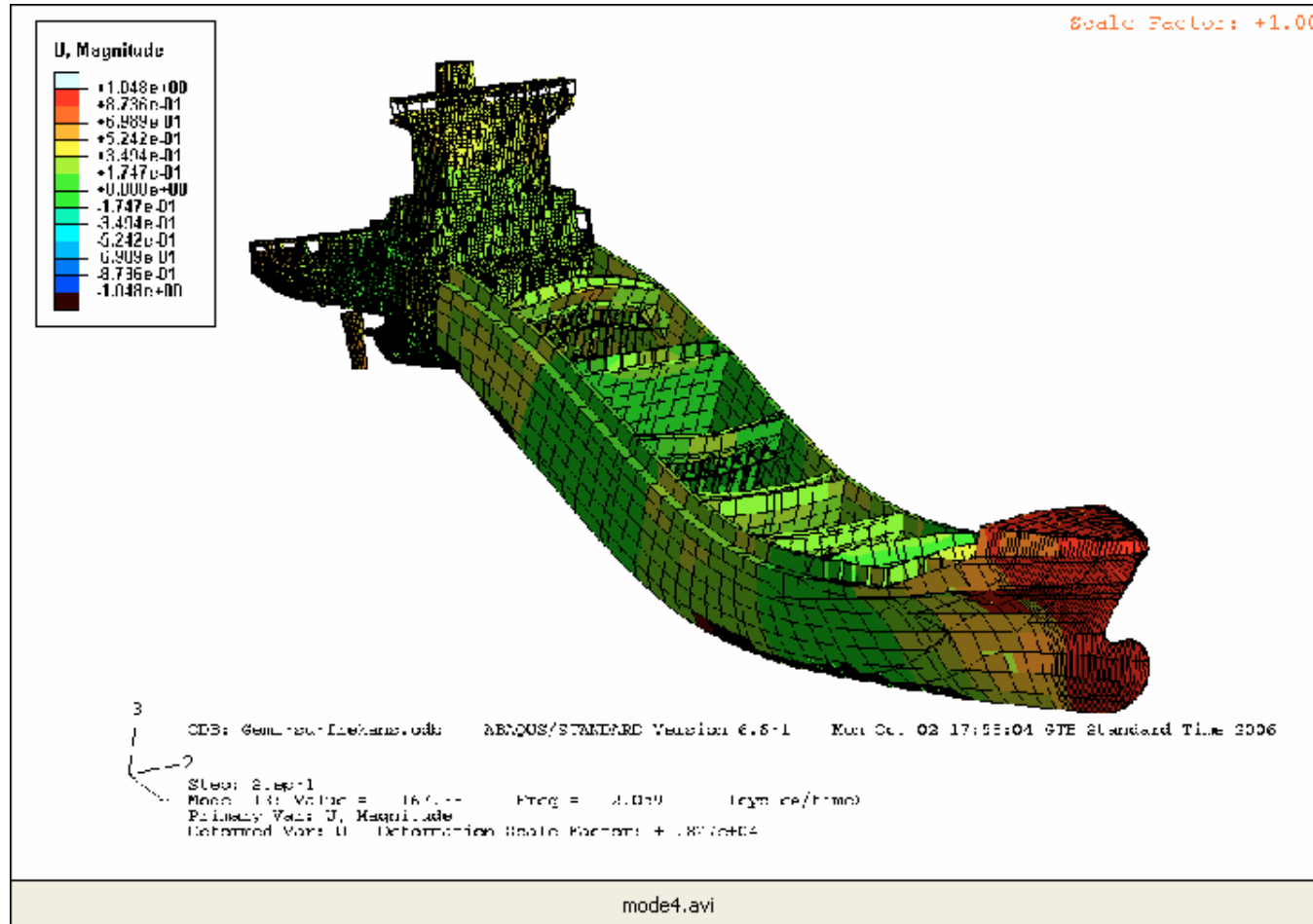
Dry Freq = 1.331 Hz



Dry Freq = 1.515 Hz

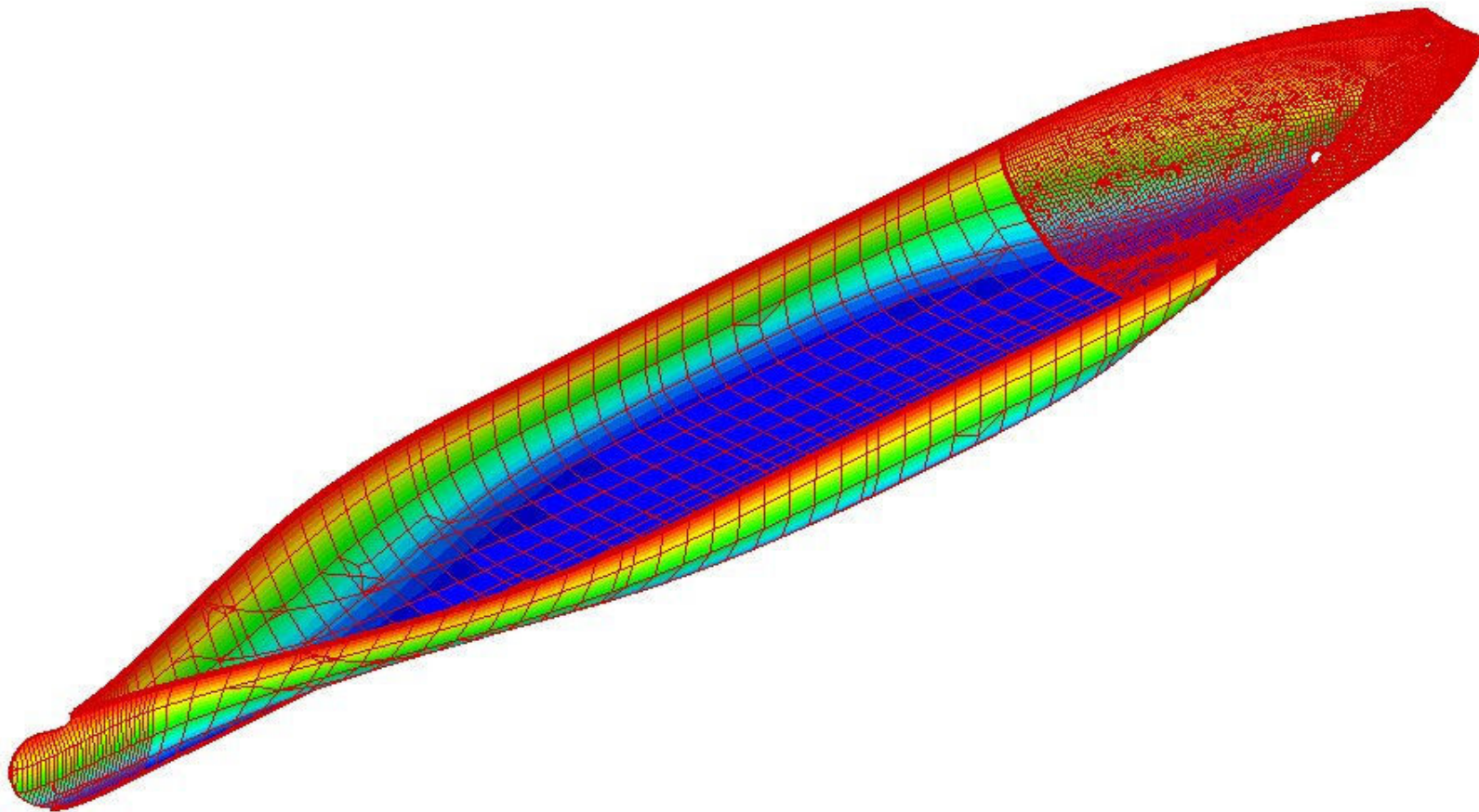


Dry Freq = 1.676 Hz



Hydroelastic Investigation of a 1900 TEU Container Ship – BE Model

- Number of nodes = 10674
 - Number of elements = 10772
- 12 in vacuo modes employed in the analysis



generalized added mass (kgm²)
 (1st ten modes, corresponding to 1 kgm² generalized structural mass)

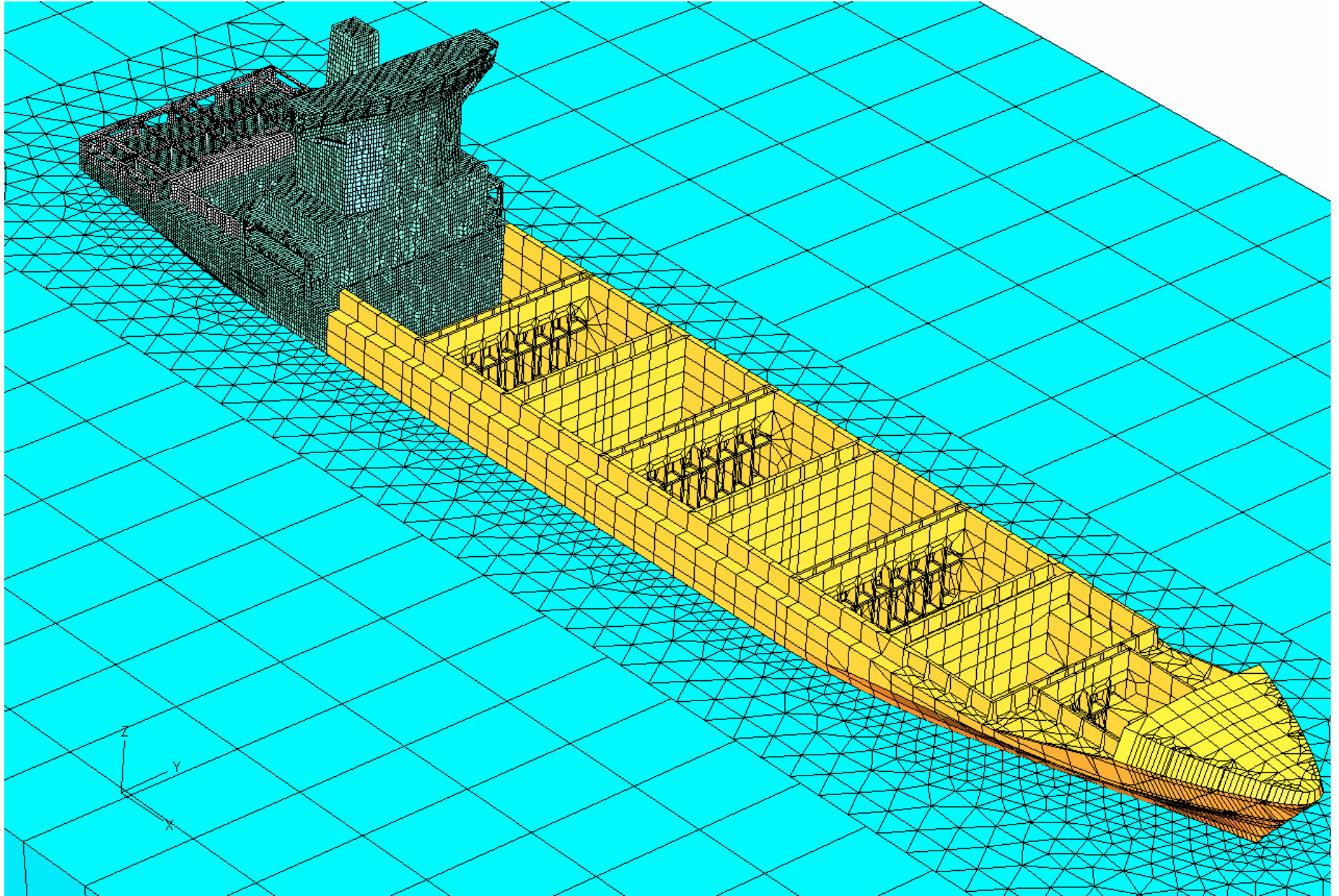
	1	2	3	4	5	6	7	8	9	10
1	0.24	0.00	0.11	0.03	0.00	-0.09	0.11	0.00	-0.01	0.00
2	0.00	0.63	0.00	0.00	-0.06	0.00	0.00	0.20	0.00	0.04
3	0.07	0.00	0.27	-0.02	0.00	0.00	0.08	0.00	0.01	0.00
4	0.03	0.00	-0.05	0.17	-0.01	0.03	-0.05	0.00	-0.02	0.00
5	0.00	-0.07	0.00	0.00	0.67	0.00	0.00	0.04	0.00	-0.01
6	-0.07	0.00	0.00	0.02	0.00	0.20	-0.08	0.00	0.02	0.00
7	0.45	0.00	0.50	-0.15	0.00	-0.38	0.58	0.00	-0.03	-0.02
8	0.00	0.32	0.00	0.00	0.05	0.00	0.00	0.49	0.00	-0.04
9	-0.01	0.00	0.01	-0.02	0.00	0.03	-0.01	0.00	0.15	0.00
10	-0.01	0.09	-0.01	0.00	-0.02	0.01	-0.01	-0.06	0.01	0.06

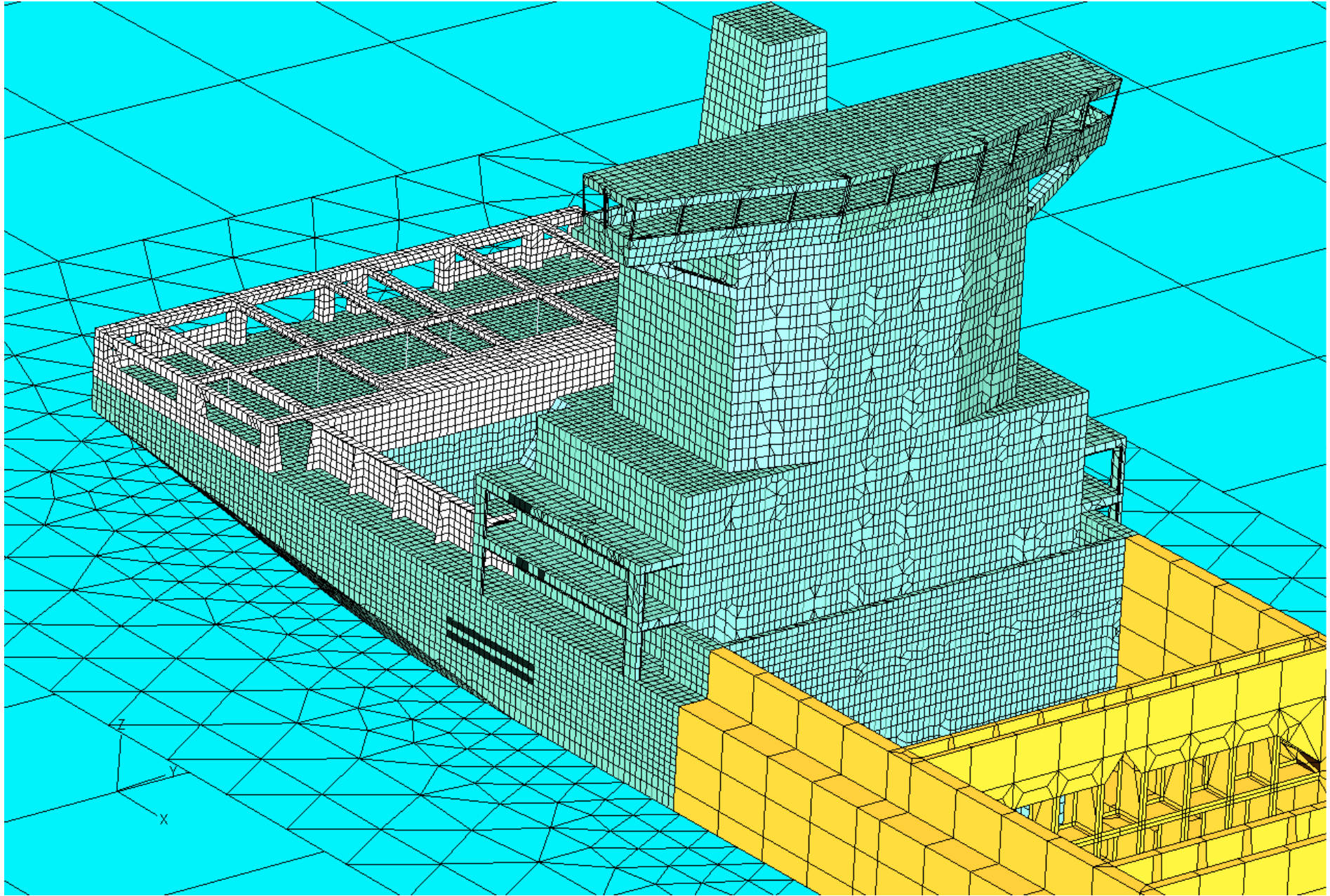
principle coordinates (1st ten modes)

	1	2	3	4	5	6	7	8	9	10
1	1.00	0.01	0.08	0.01	0.00	-0.01	0.04	0.00	0.00	0.00
2	0.01	-1.00	0.00	0.00	0.01	0.00	0.00	-0.03	0.00	-0.01
3	-0.21	0.00	0.98	-0.02	0.00	0.00	0.07	0.00	0.00	0.00
4	0.00	0.05	0.00	-0.02	1.00	0.00	0.00	0.03	0.00	-0.01
5	0.01	0.00	-0.04	-0.98	-0.01	-0.04	0.17	0.00	0.01	0.00
6	0.12	0.00	0.07	-0.15	0.00	0.36	-0.91	0.00	0.02	0.01
7	0.04	0.01	0.07	-0.05	0.00	-0.52	-0.84	-0.07	-0.01	0.01
8	0.00	0.13	-0.01	0.01	0.04	0.07	0.10	-0.96	0.01	0.07
9	0.01	0.00	-0.01	0.03	0.00	-0.04	0.03	0.01	1.00	0.02
10	0.00	0.02	0.00	0.00	-0.04	0.00	-0.01	0.02	0.01	-0.64

Hydroelastic Investigation of a 1900 TEU Container Ship – FE Wet Model

- 60300 fluid elements are used to model the behavior of fluid surrounding the ship hull.



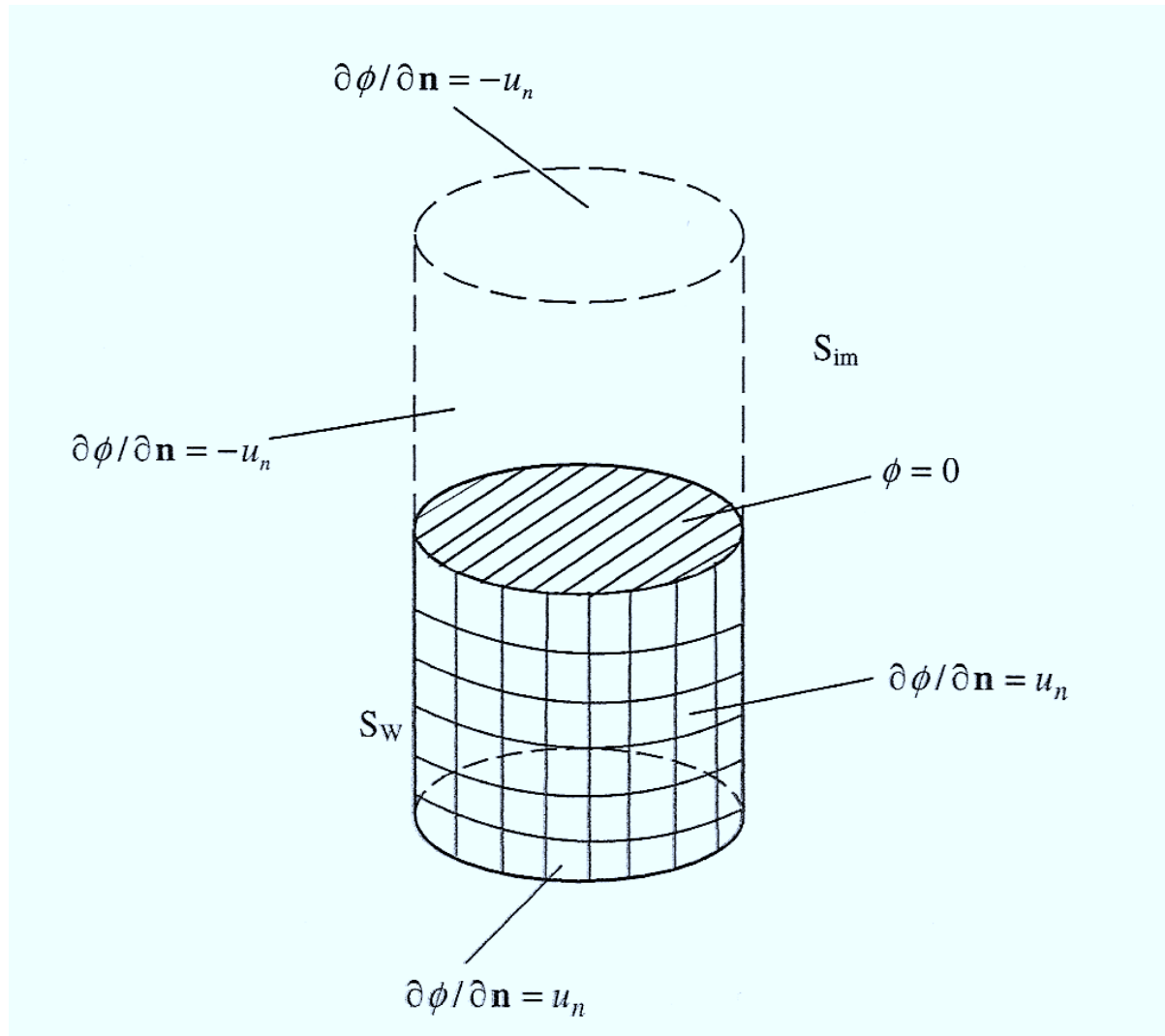


Comparison of Wet BE and FE Results

global vibration mode	wet freq (Hz)			
	dry freq (Hz)	fem	bem	err
1st torsion	1.119	0.998	0.998	0.0
1st bending	1.331	1.015	1.041	2.5
1st hor. bending & tors.	1.515	1.328	1.348	1.5
2nd torsion	2.547	2.325	2.342	0.7
2nd bending	2.676	2.059	2.071	0.6

NUMERICAL RESULTS

Fluid Storage Tanks



NUMERICAL RESULTS

Fluid Storage Tanks

Table 3

Comparisons of *dry* and *wet* natural frequencies for clamped–free cylindrical shell (Hz)

Mode (m, n)	Dry analysis			Wet analysis								
	This study	FEA [5]	Experiment [5]	$d/L = 0.5$			$d/L = 0.7$			$d/L = 1$		
				This study	FEA [5]	Experiment [5]	This study	FEA [5]	Experiment [5]	This study	FEA [5]	Experiment [5]
1,3	634.2	633	616	608.9	609.4	542.0	543.1	522	400.7	400.6	388	
1,2	814.2	814	708	769.3	771.1	669.8	672.7	582	481.1	482.1	421	
1,4	949.2	947	945	908.4	908.8	806.8	806.0	798	635.3	633.2	628	
1,5	1482.5	1480	1479	1351.8	1352.8	1195.5	1188.4	1196	1039.7	1033.0	1027	
2,4	1649.8	1648	1628	1308.4	1303.9	1261.4	1253.2	1244	1111.8	1110.6	1094	
1,1	1825.6	1827	—	1654.7	1654.4	1407.3	1407.4	—	1041.9	1038.6	—	
2,5	1840.3	1839	1851	1571.3	1565.8	1557.7	1553.8	1546	1305.0	1304.2	1299	
2,3	2029.9	2029	1969	1519.9	1515.2	1434.0	1425.3	1394	1288.0	1286.9	1245	
1,6	2156.8	2154	2151	1843.5	1842.7	1693.6	1679.7	—	1574.3	1561.3	1546	
2,6	2385.8	—	—	2189.6	2189.0	2119.7	—	—	1762.4	1762.6	1748	

[5] T. Mazúch, J. Horáček, J. Trnka, J. Veselý, Natural modes and frequencies of a thin clamped-free cylindrical storage tank partially filled with water: FEM and measurements, *Journal of Sound and Vibration*, Vol.193, pp.669-690, 1996

NUMERICAL RESULTS

Fluid Storage Tanks

A. Ergin, B. Uğurlu / Journal of Sound and Vibration 275 (2004) 489–513

501

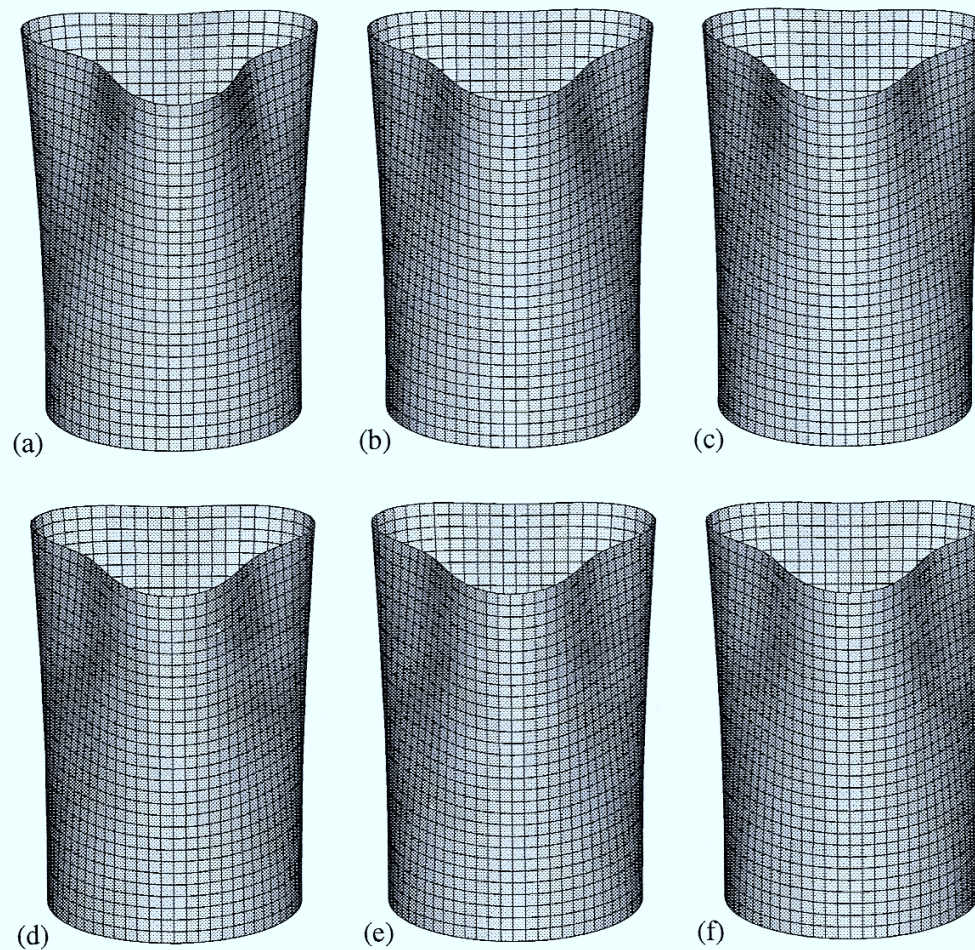


Fig. 4. Predicted mode shapes with $m = 1$ and $n = 3$: (a) empty shell, $d/L = 0$; (b) $d/L = 0.2$; (c) $d/L = 0.4$; (d) $d/L = 0.6$; (e) $d/L = 0.8$; (f) $d/L = 1$.

NUMERICAL RESULTS

Fluid Storage Tanks

502

A. Ergin, B. Uğurlu / Journal of Sound and Vibration 275 (2004) 489–513

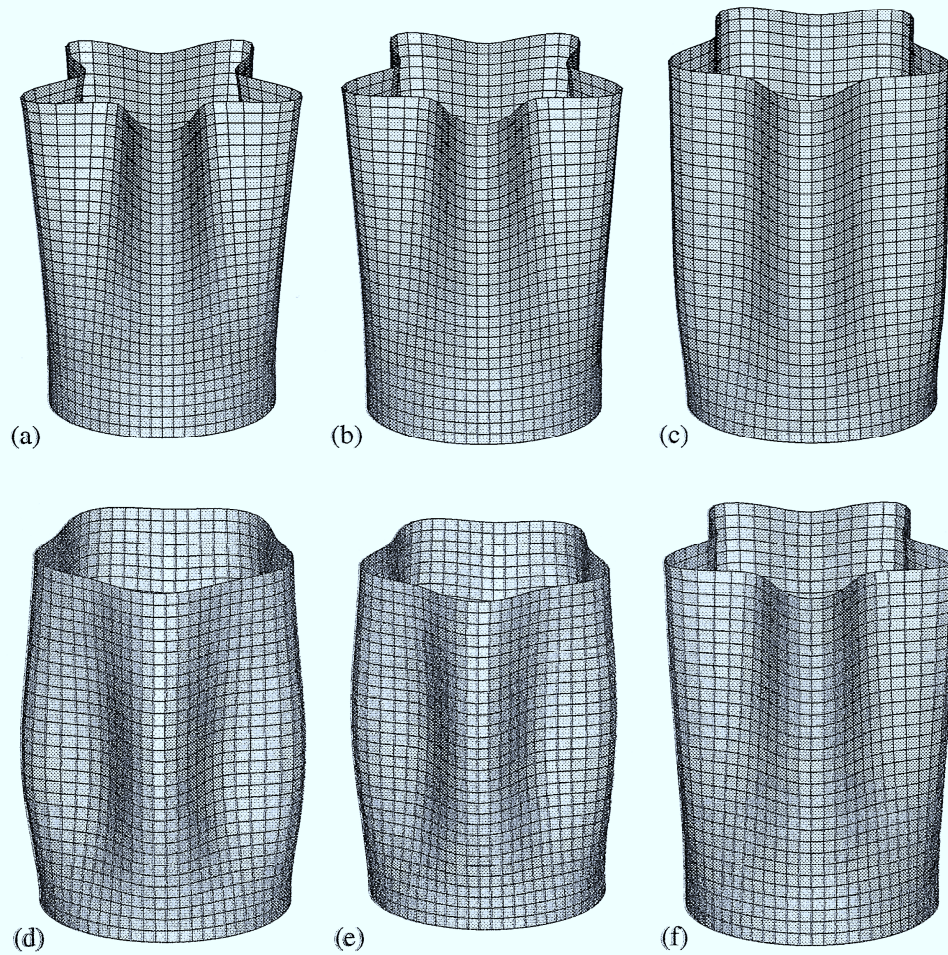


Fig. 5. Predicted mode shapes with $m = 1$ and $n = 5$: (a) empty shell, $d/L = 0$; (b) $d/L = 0.2$; (c) $d/L = 0.4$; (d) $d/L = 0.6$; (e) $d/L = 0.8$; (f) $d/L = 1$.

NUMERICAL RESULTS

Fluid Storage Tanks

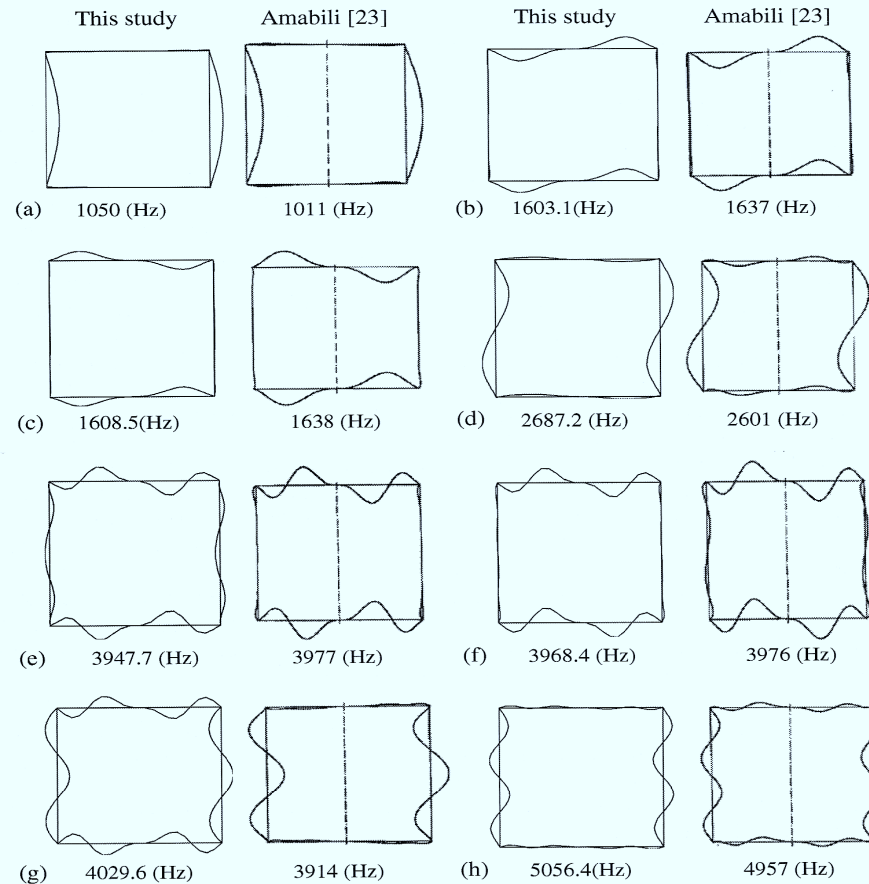


Fig. 7. Comparisons of predicted wet mode shapes of completely filled hermetic can for n (or i) = 3: (a) first symmetric shell-dominant mode; (b) first anti-symmetric plate-dominant mode; (c) first symmetric plate-dominant mode; (d) first anti-symmetric shell-dominant mode; (e) second symmetric plate-dominant mode; (f) second anti-symmetric plate-dominant mode; (g) second symmetric shell-dominant mode; (h) second anti-symmetric shell-dominant mode.

NUMERICAL RESULTS

Elastic Structure Containing Axial Flow

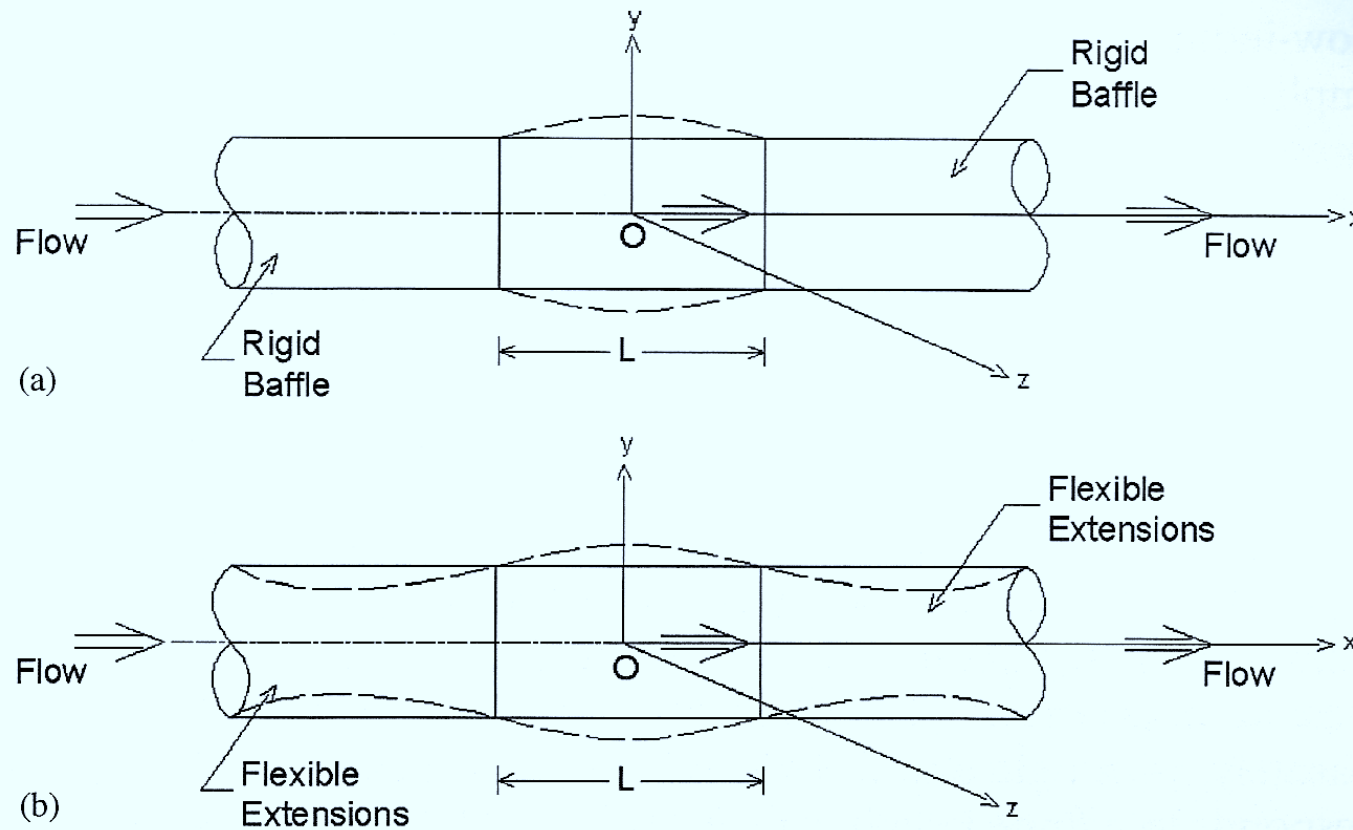


Fig. 1. Cylindrical shell conveying flowing fluid, (a) with rigid extensions and (b) with flexible extensions.

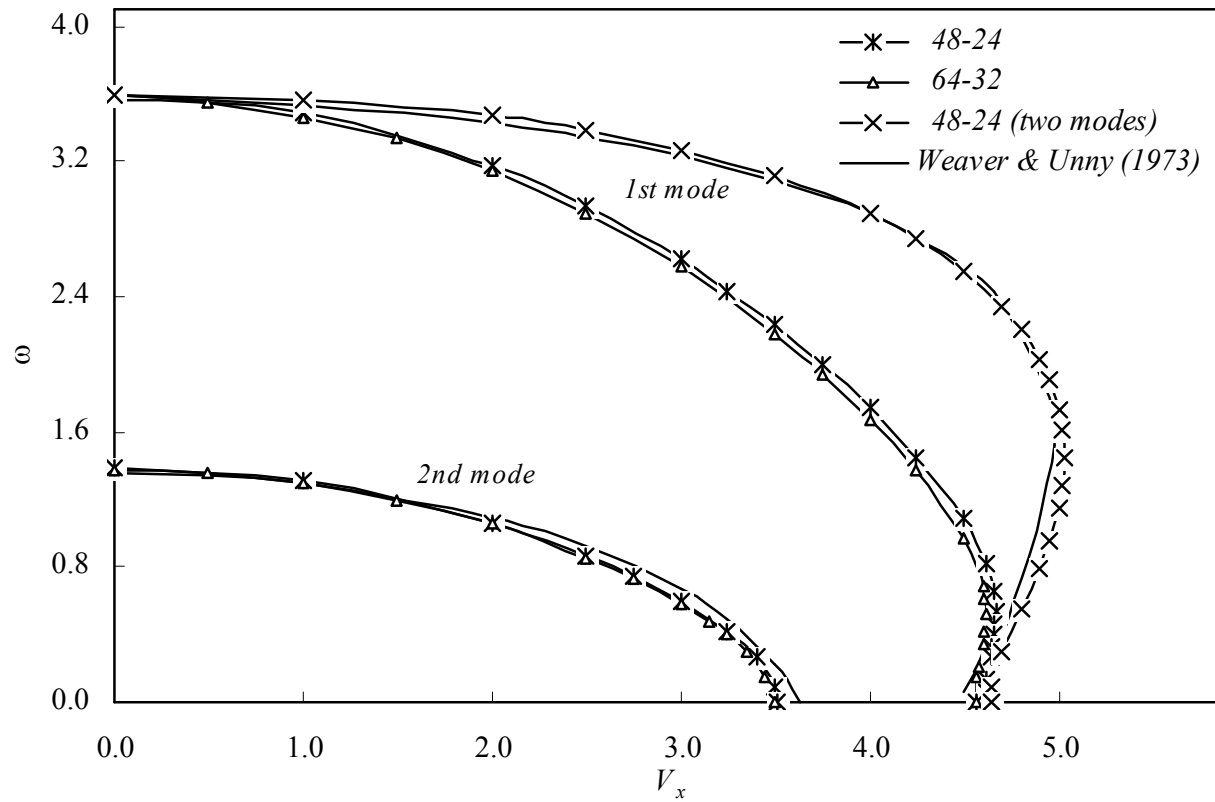
NUMERICAL RESULTS

Elastic Structure Containing Axial Flow

The structure adopted for calculations is a finite length cylindrical shell, simply supported at both ends, and it was analytically investigated by Weaver and Unny (1973), Selmane and Lakis (1997), Amabili *et al* (1999) and Amabili and Garziera (2002). The shell structure has the geometric and material properties: length-to-radius ratio $L/R = 2$, thickness-to-radius ratio $h/R = 0.01$, Young's modulus $E = 206$ GPa, Poisson's ratio $\nu = 0.3$, and mass density $\rho_s = 7850$ kg/m³. Fresh water is used as the contained fluid with a density of $\rho_f = 1000$ kg/m³.

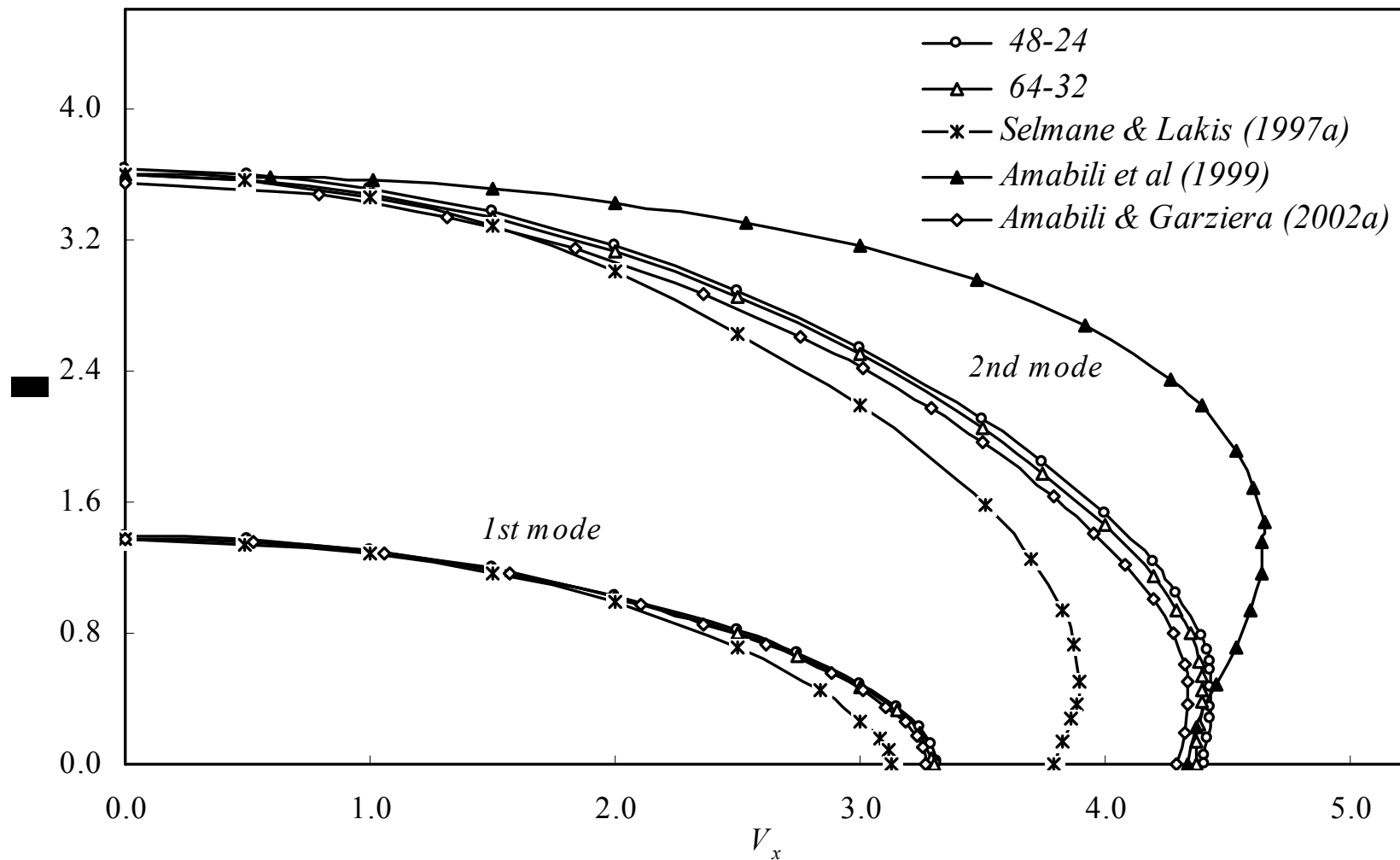
NUMERICAL RESULTS

Elastic Structure Containing Axial Flow



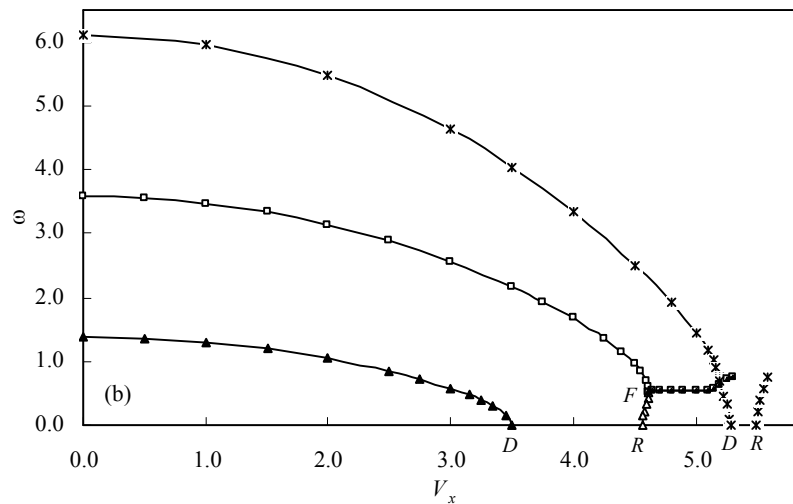
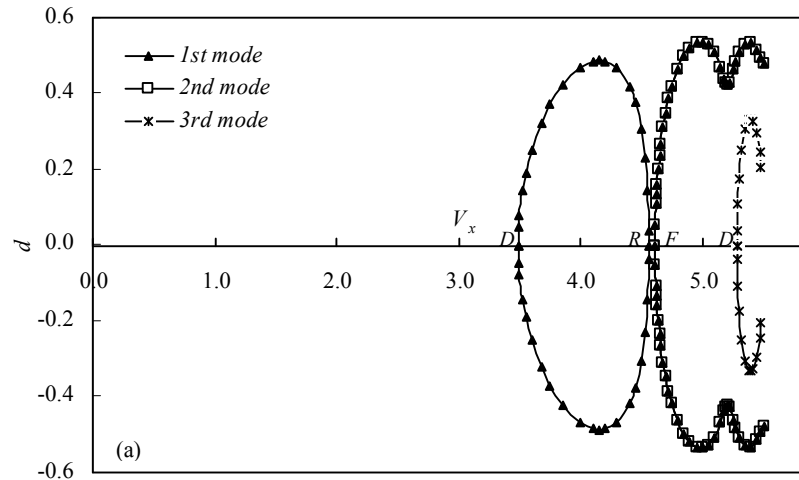
NUMERICAL RESULTS

Elastic Structure Containing Axial Flow



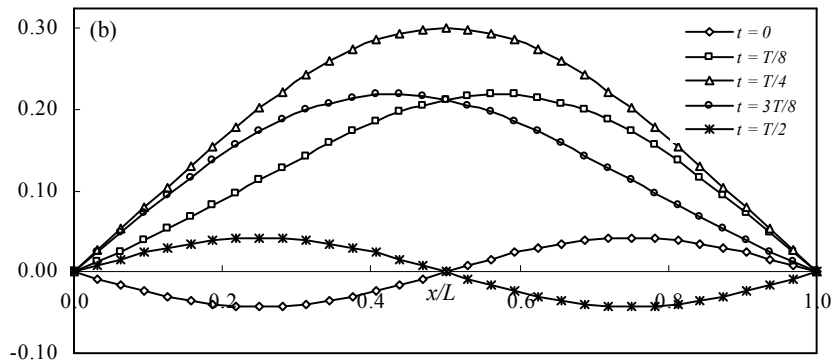
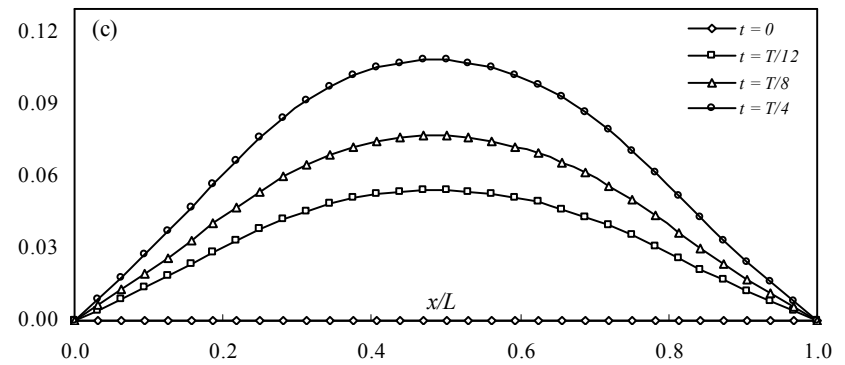
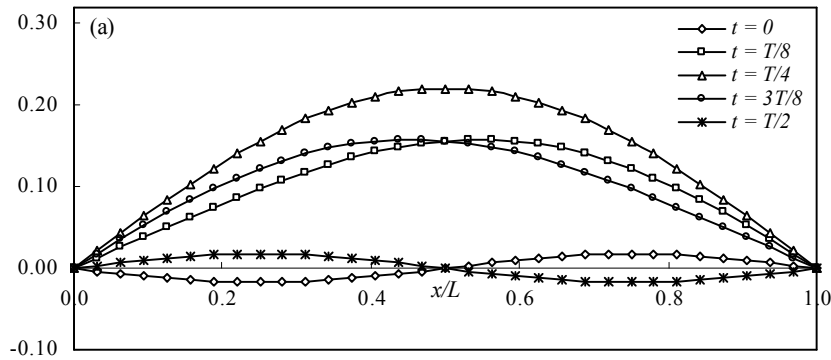
NUMERICAL RESULTS

Elastic Structure Containing Axial Flow



NUMERICAL RESULTS

Elastic Structure Containing Axial Flow



Conclusions

- It can also be said that the hybrid method introduced in this study can be applied to any shape of cylindrical structure partially in contact with internal and/or external flowing fluid, in contrast to the studies found in the literature.
- The present study has demonstrated the versatility of the method developed before and extended in this study further. By introducing the linearly varying boundary elements in this study, the convergence of the numerical predictions were obtained much faster than those using constant distributions over the boundary elements.
- the predicted frequency values behave as expected. It is to say that they decrease with increasing non-dimensional axial flow velocity, and they reach a zero frequency for the axial flow velocity at which a static divergence occurs.

Hydro-Elastic Analysis of Marine Structures Using a Boundary Integral Equation Method

L. Kaydıhan², B. Uğurlu¹ and A. Ergin¹

¹ Faculty of Naval Architecture and Ocean Eng., ITU,
Turkey

² Delta Marine, Turkey

Hydroelasticity Research Group in ITU

Professor A. Ergin, ITU

Dr. B. Uğurlu, ITU

L. Kaydıhan, DELTA MARINE TURKEY

S.A. Köroğlu, ITU

Activities of Research Group

- General 3D Hydroelasticity Method
- Experimental studies; modal analysis, operational modal analysis, vibration measurements
- Outcomes are reported in *Journal of Sound and Vibration* and *Journal of Fluids and Structures*
- Research Projects founded by *Technical Research Council of Turkey*

MATHEMATICAL MODEL

Fluid – Structure Interaction Problem

The fluid is assumed ideal, i.e., inviscid and incompressible, and its motion is irrotational and there exists a fluid velocity vector, \mathbf{v} , which can be defined as the gradient of the velocity potential function Φ as

$$\mathbf{v}(x, y, z, t) = \nabla \Phi(x, y, z, t) \quad (1)$$

The velocity potential Φ may be expressed as

$$\Phi = U x + \phi \quad (2)$$

MATHEMATICAL MODEL

Fluid – Structure Interaction Problem

Here the steady velocity potential U represents the effect of the mean flow associated with the undisturbed flow velocity U in the Axial direction. Further, ϕ is the unsteady velocity potential associated with the perturbations to the flow field due to the motion of the flexible body and satisfies the Laplace equation

$$\nabla^2 \phi = 0 \quad (3)$$

throughout the fluid domain. For the structure immersed in and/or containing flowing fluid, the vibratory response of the structure may be expressed in terms of principal coordinates as

$$\mathbf{p}(t) = \mathbf{p}_0 e^{\lambda t} \quad (4)$$

MATHEMATICAL MODEL

Fluid – Structure Interaction Problem

The velocity potential function due to the distortion of the structure in the r th *in vacuo* vibrational mode may be written as follows

$$\phi_r(x, y, z, t) = \phi_r(x, y, z) p_{0r} e^{\lambda t} \quad (5)$$

where M represents the number of modes of interest, and p_{0r} is an unknown complex amplitude for the r th principal coordinate.

On the wetted surface of the vibrating structure the normal fluid velocity must equal to the normal velocity on the structure and this condition for the r th modal vibration of the elastic structure containing and/or submerged in flowing fluid can be expressed as

$$\frac{\partial \phi_r}{\partial n} = \left(\frac{\partial \mathbf{u}_r}{\partial t} + U \frac{\partial \mathbf{u}_r}{\partial x} \right) \cdot \mathbf{n} \quad (6)$$

MATHEMATICAL MODEL

Fluid – Structure Interaction Problem

The vector \mathbf{u}_r denotes the displacement response of the structure in the r th principal coordinate and it may be written as

$$\mathbf{u}_r(x, y, z, t) = \mathbf{u}_r(x, y, z) p_{0r} e^{\lambda t} \quad (7)$$

Substituting Eqs. (5) and (7) into (6), the following expression is obtained for the boundary condition on the fluid-structure interface

$$\frac{\partial \phi_r}{\partial \mathbf{n}} = \lambda \mathbf{u}_r(x, y, z) \cdot \mathbf{n} + U \frac{\partial \mathbf{u}_r(x, y, z)}{\partial x} \cdot \mathbf{n} \quad (8)$$

MATHEMATICAL MODEL

Fluid – Structure Interaction Problem

It is assumed that the elastic structure vibrates at relatively high frequencies so that the effect of surface waves can be neglected. Therefore, the free surface condition (infinite frequency limit condition) for the perturbation potential can be approximated by

$$\phi_r = 0 \quad \text{on the free surface} \quad (9)$$

The method of images may be used to satisfy this boundary condition. By adding an imaginary boundary region, the condition given by Eq. (9) at the horizontal surface can be omitted; thus the problem is reduced to a classical Neumann case. It should be noted that, for the completely filled elastic structure, the normal fluid velocity cannot be arbitrarily specified. It has to satisfy the incompressibility condition

$$\iint_{S_w + S_{im}} \frac{\partial \phi_r}{\partial \mathbf{n}} dS = 0, \quad (10)$$

MATHEMATICAL MODEL

Numerical Evaluation of Perturbation Potential

The boundary value problem for the perturbation potential, may be expressed in the following form:

$$c(\xi)\phi(\xi) = \iint_{S_w} (\phi^*(s, \xi)q(s) - \phi(s)q^*(s, \xi)) dS \quad (11)$$

where ξ and s denote, respectively, the evaluation and field points on the wetted surface. ϕ^* is the fundamental solution and expressed as follows,

$$\phi^*(s, \xi) = \frac{1}{4\pi r} \quad (12)$$

MATHEMATICAL MODEL

Numerical Evaluation of Perturbation Potential

$q = \partial \phi / \partial \mathbf{n}$ is the flux, and r the distance between the evaluation and field points. The free term is defined as the fraction of that lies inside the domain of interest. Moreover, $q^*(s, \xi)$ can be written as

$$q^*(s, \xi) = -(\partial r / \partial \mathbf{n}) / 4 \pi r^3 \quad (13)$$

The fluid-structure interaction problem may be separated into two parts: (i) the vibration of the elastic structure in a quiescent fluid, and (ii) the disturbance in the main axial flow due to the oscillation of the structure. Thus, defining ϕ , Eq (7) may be divided into two separate parts as

$$\frac{\partial \phi_1}{\partial \mathbf{n}} = \mathbf{u}(x, y, z) \cdot \mathbf{n}, \quad \frac{\partial \phi_2}{\partial \mathbf{n}} = \frac{\partial \mathbf{u}(x, y, z)}{\partial x} \cdot \mathbf{n}, \quad (14a,b)$$

MATHEMATICAL MODEL

Numerical Evaluation of Perturbation Potential

For the solution of Eq. (11) with boundary conditions (14a and b), the wetted surface can be idealized by using boundary elements, referred to as hydrodynamic panels, and the distribution of the potential function and its flux over each hydrodynamic panel may be described in terms of the shape functions and nodal values as

$$\phi_e = \sum_{j=1}^{n_e} N_{ej} \phi_{ej}, \quad q_e = \sum_{j=1}^{n_e} N_{ej} q_{ej} \quad (15)$$

Here, n_e represents the number of nodal points assigned to each hydrodynamic panel, and N_{ej} the shape function adopted for the distribution of the potential function. e and j indicates the numbers of the hydrodynamic panels and nodal points, respectively.

MATHEMATICAL MODEL

Numerical Evaluation of Perturbation Potential

In the case of a linear distribution adopted in this study, the shape functions for a quadrilateral panel may be expressed as

$$N_{e1} = ((1 - \zeta)(1 - \eta)) / 4$$

$$N_{e2} = ((1 + \zeta)(1 - \eta)) / 4$$

$$N_{e3} = ((1 + \zeta)(1 + \eta)) / 4$$

$$N_{e4} = ((1 - \zeta)(1 + \eta)) / 4$$

(16)

MATHEMATICAL MODEL

Numerical Evaluation of Perturbation Potential

After substituting Eqs. (15) and (16) into Eq. (11) and applying the boundary conditions given in Eqs. (14a) and (14b), the unknown potential function values can be determined from the following sets of algebraic equations

$$c_k \phi_{1k} + \sum_{i=1}^m \sum_{j=1}^{n_m} (\phi_{1ij} \iint_{\Delta S_i} N_j q^* dS = \sum_{i=1}^m \sum_{j=1}^{n_m} (\mathbf{u}_{ij} \cdot \mathbf{n}_j \iint_{\Delta S_i} N_j \phi^* dS), \quad (17 a)$$

$$c_k \phi_{2k} + \sum_{i=1}^m \sum_{j=1}^{n_m} (\phi_{2ij} \iint_{\Delta S_i} N_j q^* dS = \sum_{i=1}^m \sum_{j=1}^{n_m} \left(\frac{\partial \mathbf{u}_{ij}}{\partial x} \cdot \mathbf{n}_j \iint_{\Delta S_i} N_j \phi^* dS \right),$$

$$k = 1, 2, \dots, m$$

where m denotes the number of nodal points used in the discretization of the structure

MATHEMATICAL MODEL

Calculation of Generalized Fluid-Structure Interaction Force Coefficients

Using the Bernoulli's equation and neglecting the second order terms, the dynamic fluid pressure on the elastic structure due to the r th modal vibration becomes

$$P_r(x, y, z, t) = -\rho \left(\frac{\partial \phi_r}{\partial t} + U \frac{\partial \phi_r}{\partial x} \right), \quad (18)$$

Substituting equation (5) into (18), the following expression for the pressure is obtained,

$$P_r(x, y, z, t) = -\rho \left(\lambda \phi_r + U \frac{\partial \phi_r}{\partial x} \right) p_{0r} e^{\lambda t}. \quad (19)$$

MATHEMATICAL MODEL

Calculation of Generalized Fluid-Structure Interaction Force Coefficients

By using the definition of $\phi_r = \lambda \phi_{r1} + U \phi_{r2}$, equation (19) may be rewritten in the following form:

$$P_r(x, y, z, t) = -\rho (\lambda^2 \phi_{r1} + U \lambda (\frac{\partial \phi_{r1}}{\partial x} + \phi_{r2}) + U^2 \frac{\partial \phi_{r2}}{\partial x}) p_{0r} e^{\lambda t} \quad (20)$$

The *kth* component of the generalized fluid-structure interaction force due to the *rth* modal *in-vacuo* vibration of the elastic structure subjected to axial flow can be expressed in terms of the pressure acting on the wetted surface of the structure as

MATHEMATICAL MODEL

Calculation of Generalized Fluid-Structure Interaction Force Coefficients

$$\begin{aligned} Z_{kr} &= \iint_{S_w} P_r(x, y, z, t) \mathbf{u}_k \mathbf{n} dS \\ &= -p_{0r} e^{\lambda t} \iint_{S_w} \rho \left(\lambda^2 \phi_{r1} + U \lambda \left(\frac{\partial \phi_{r1}}{\partial x} + \phi_{r2} \right) + U^2 \frac{\partial \phi_{r2}}{\partial x} \right) \mathbf{u}_k \mathbf{n} dS \\ &= -\lambda^2 p_{0r} e^{\lambda t} \rho \iint_{S_w} \phi_{r1} \mathbf{u}_k \mathbf{n} dS - \lambda p_{0r} e^{\lambda t} \rho U \iint_{S_w} \left(\frac{\partial \phi_{r1}}{\partial x} + \phi_{r2} \right) \mathbf{u}_k \mathbf{n} dS \\ &\quad - p_{0r} e^{\lambda t} \rho U^2 \iint_{S_w} \frac{\partial \phi_{r2}}{\partial x} \mathbf{u}_k \mathbf{n} dS \end{aligned} \tag{21}$$

MATHEMATICAL MODEL

Calculation of Generalized Fluid-Structure Interaction Force Coefficients

The generalized added mass, A_{kr} , generalized fluid damping (due to the Coriolis effect of fluid), B_{kr} and generalized fluid stiffness (due to the centrifugal effect of fluid), C_{kr} terms can be defined as

$$A_{kr} = \rho \iint_{S_w} \phi_{r1} \mathbf{u}_k \mathbf{n} dS, \quad (22)$$

$$B_{kr} = \rho U \iint_{S_w} \left(\frac{\partial \phi_{r1}}{\partial x} + \phi_{r2} \right) \mathbf{u}_k \mathbf{n} dS, \quad (23)$$

$$C_{kr} = \rho U^2 \iint_{S_w} \frac{\partial \phi_{r2}}{\partial x} \mathbf{u}_k \mathbf{n} dS. \quad (24)$$

MATHEMATICAL MODEL

Calculation of Generalized Fluid-Structure Interaction Force Coefficients

Therefore, the generalized fluid-structure interaction force component, Z_{kr} , can be written as

$$\begin{aligned} Z_{kr}(t) &= -A_{kr} \lambda^2 p_{0r} e^{\lambda t} - B_{kr} \lambda p_{0r} e^{\lambda t} - C_{kr} p_{0r} e^{\lambda t} \\ &= -A_{kr} \ddot{p}_r(t) - B_{kr} \dot{p}_r(t) - C_{kr} p_r(t) \end{aligned} \quad (25)$$

MATHEMATICAL MODEL

Calculation of Wet Frequencies and Mode Shapes

The generalized equation of motion for the elastic structure in contact with axial flow assuming free vibrations with no structural damping is

$$\left[\lambda^2 (\mathbf{a} + \mathbf{A}) + \lambda (\mathbf{B}) + (\mathbf{c} + \mathbf{C}) \right] \mathbf{p} = 0, \quad (26)$$

where \mathbf{a} and \mathbf{c} denote the generalized structural mass and stiffness matrices, respectively, and they are calculated by using a standard finite element program [21]. The matrices \mathbf{A} , \mathbf{B} and \mathbf{C} represent the generalized added mass, generalized fluid damping and generalized fluid stiffness matrices, respectively.

Hydroelastic Investigation of a 1900 TEU Container Ship

MAIN PARTICULARS

Length overall	:	182.85 m
Length perpendicular	:	171.00 m
Breadth (moulded)	:	28.00 m
Depth (moulded)	:	16.10 m
Design draught	:	10.00 m
Scantling draught	:	11.00 m
Service speed	:	19.50 knot
Deadweight (at scantling draught)	:	26200 ton

1900 TEU CONTAINER SHIP

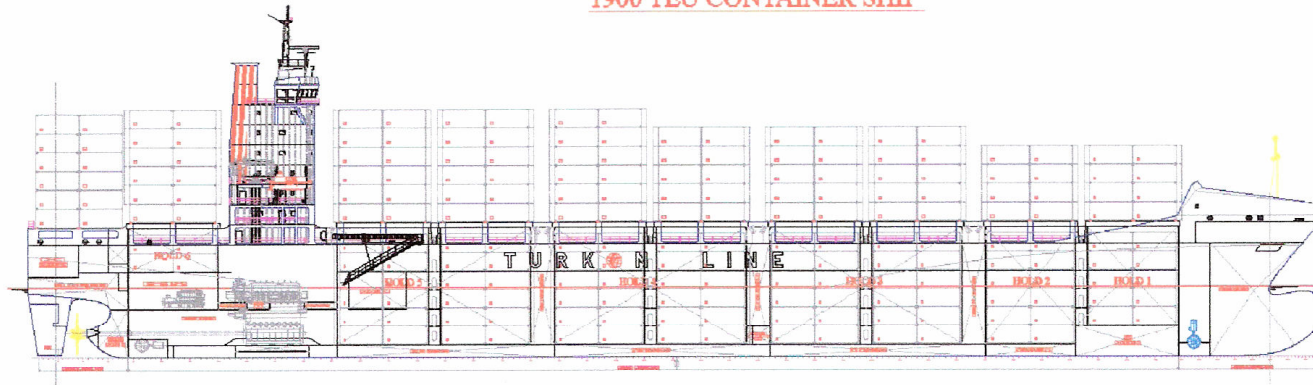


Figure 1 – General arrangement

Hydroelastic Investigation of a 1900 TEU Container Ship – FE Model

- FE calculations were carried out by Delta Marine, Turkey.
- Abaqus employed for the FE calculations
- Ship Model is developed in two parts;
Aft part consists of engine room, poop deck, aft peak and Superstructure decks.
Fore part consists of cargo area, fore peak, forecastle deck
- Fine mesh density is used for the aft part model

Hydroelastic Investigation of a 1900 TEU Container Ship – FE Model

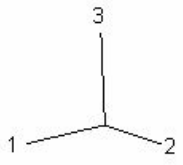
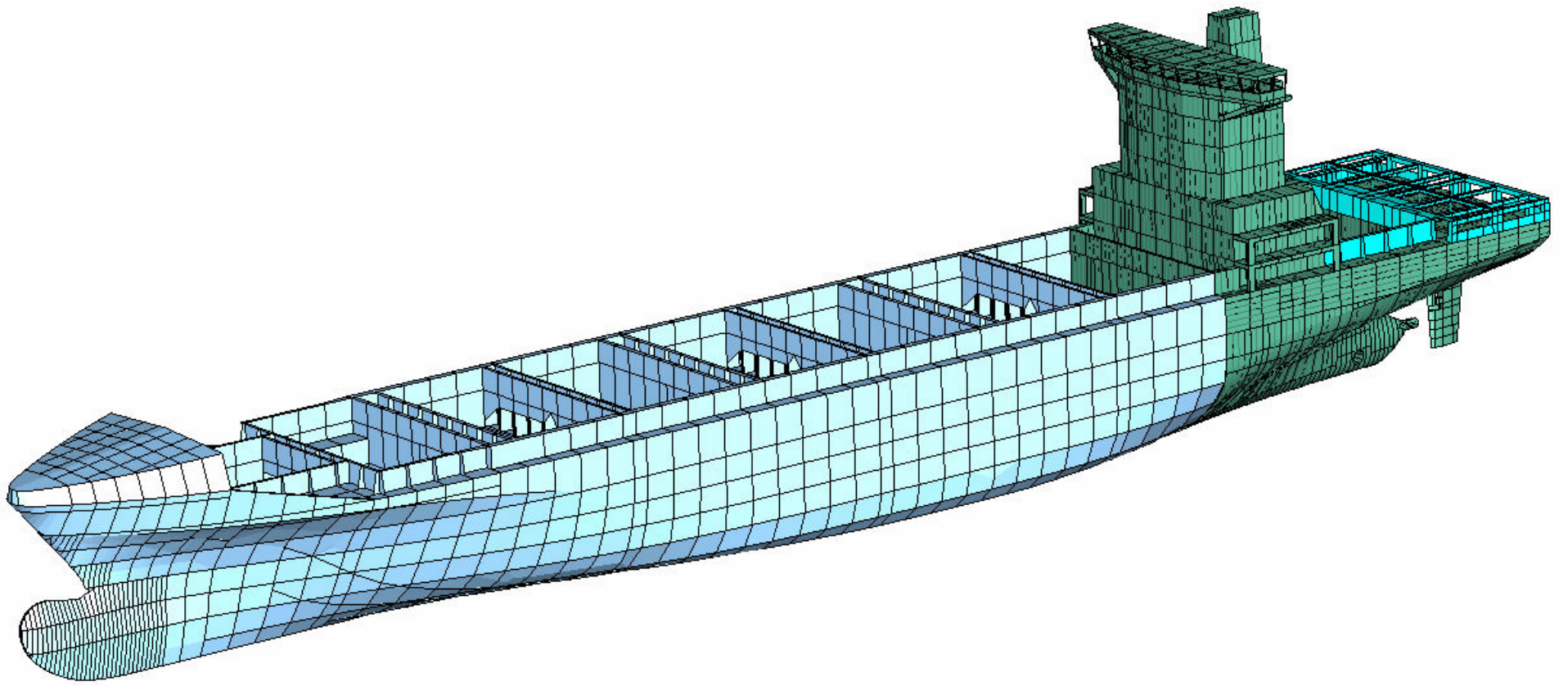
- Cargo loading is applied as inertia mass elements distributed over the cargo area inner bottom plating
- Ballast weights, heavy fuel oil and other tank weights are also applied as inertial mass elements.
- Finite elements model has 176030 nodes, 176800 structural elements

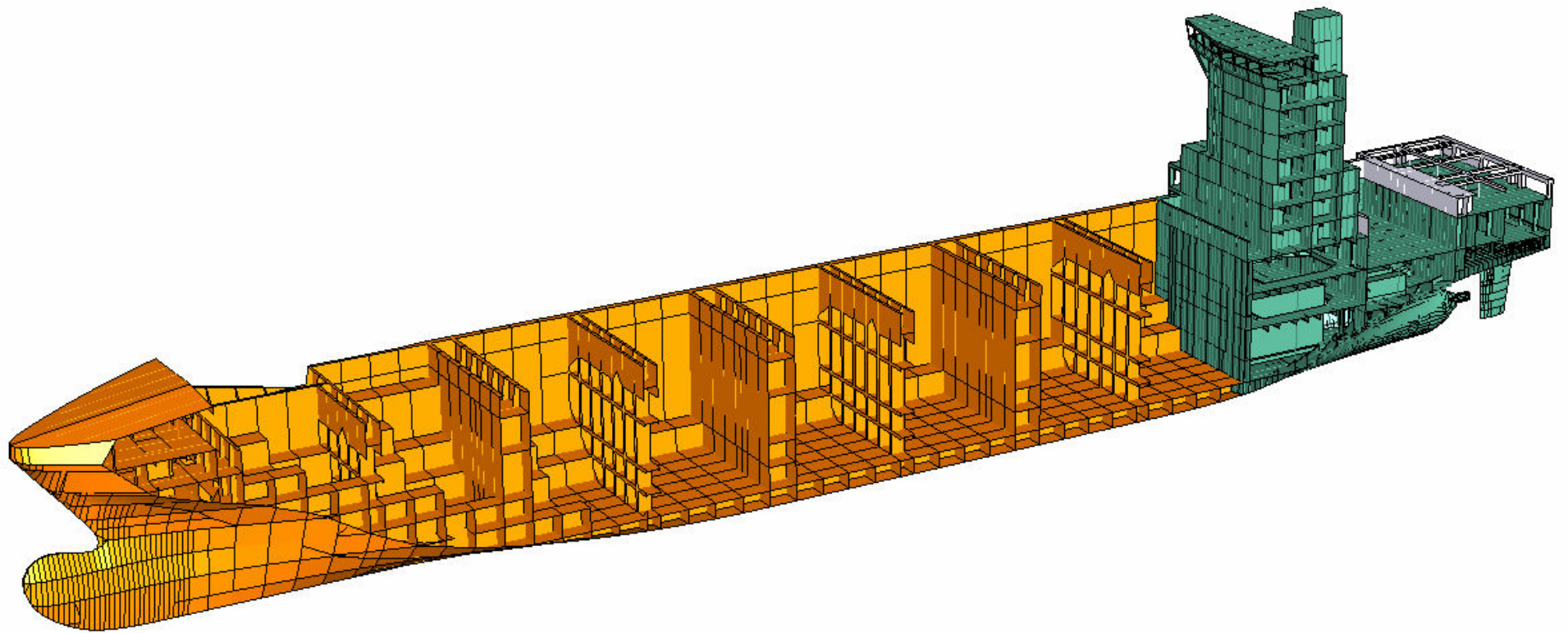
Hydroelastic Investigation of a 1900 TEU Container Ship – FE Model – Loading Cond.

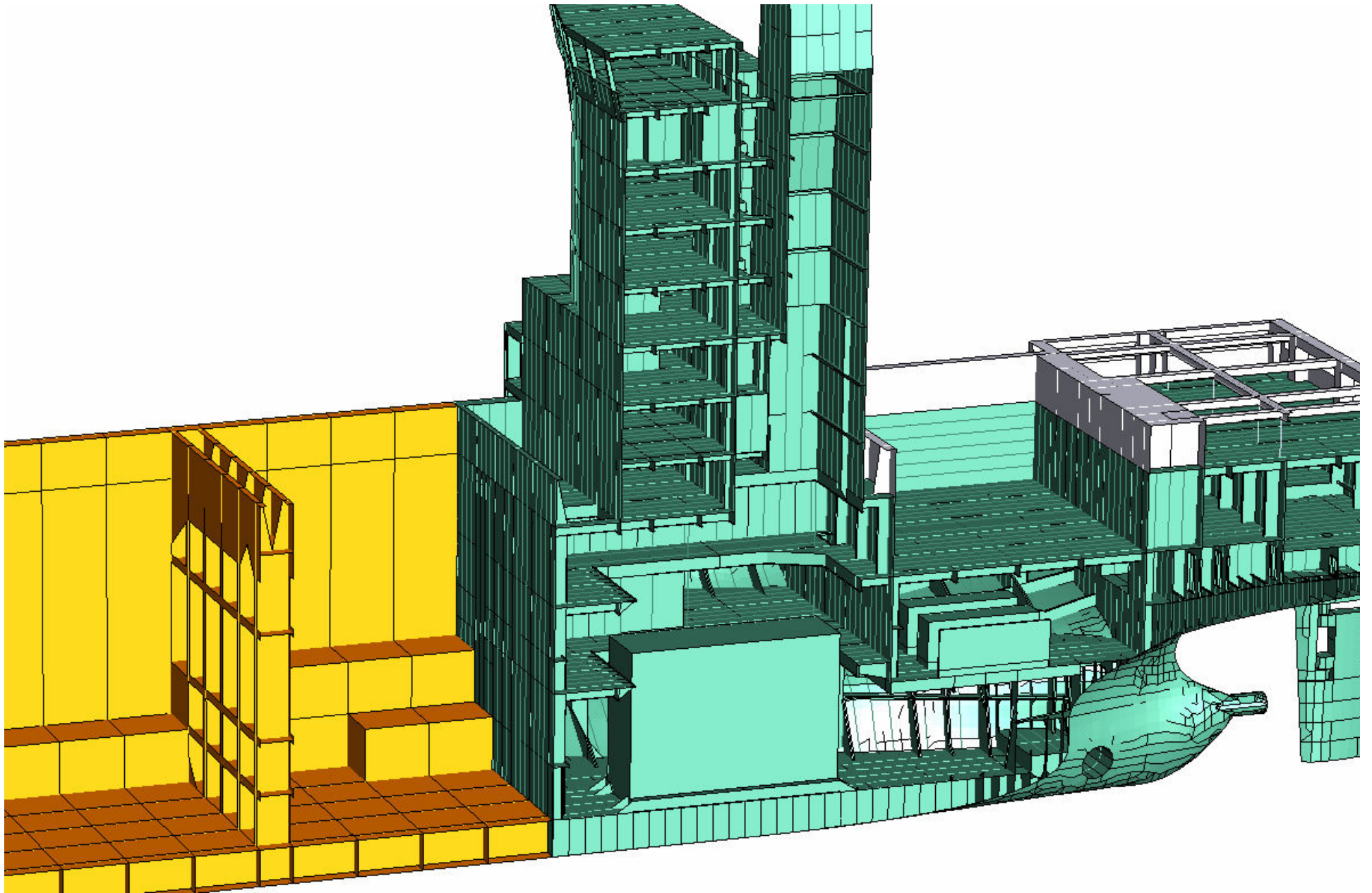
- Full loading with design draught of 10 m.
- Cargo loading – 17150 t
- Ballast weight – 3021 t
- Heavy fuel oil – 1886 t
- Marine diesel oil – 165 t
- Fresh water – 206 t
- Other tank weights – 165 t

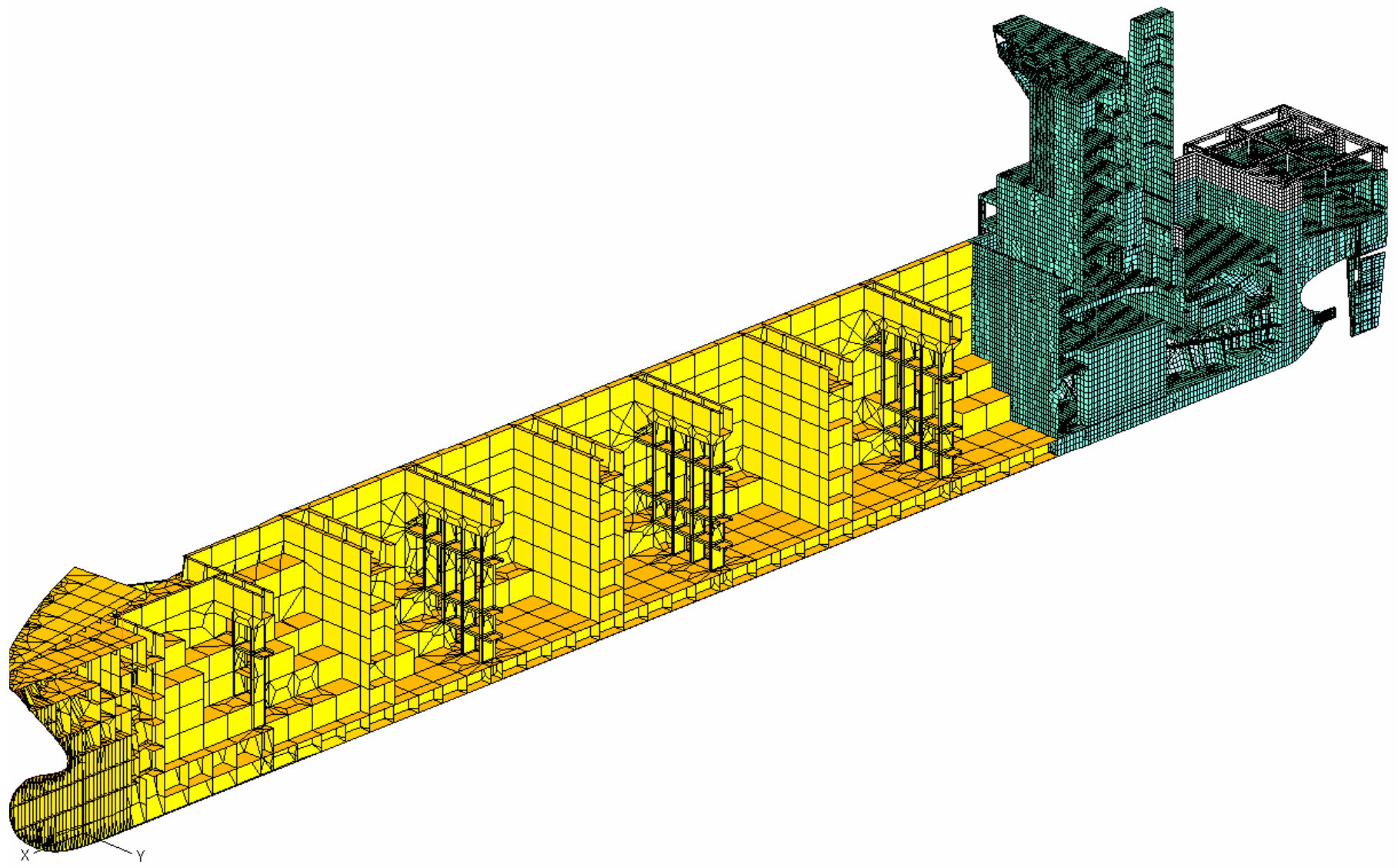
Hydroelastic Investigation of a 1900 TEU Container Ship – FE Model – Loading Cond.

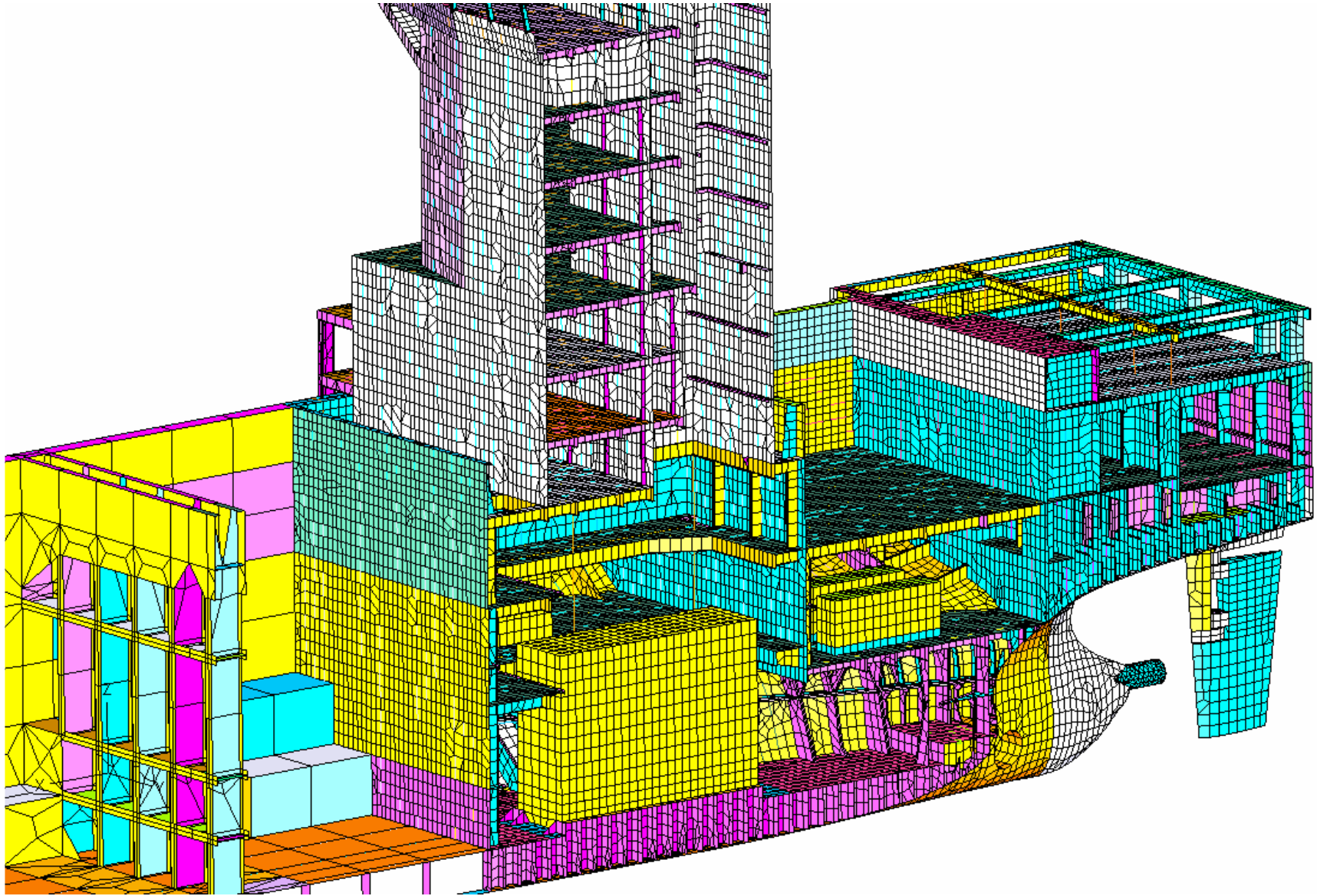
- LWT – 9000 t
- DWT – 22595.7 t
- Total Weight – 31595.7 t
- Total Finite Element Weight – 31520 t
- LCG – 79.85 m
- LCG – FEM – 80.3 m



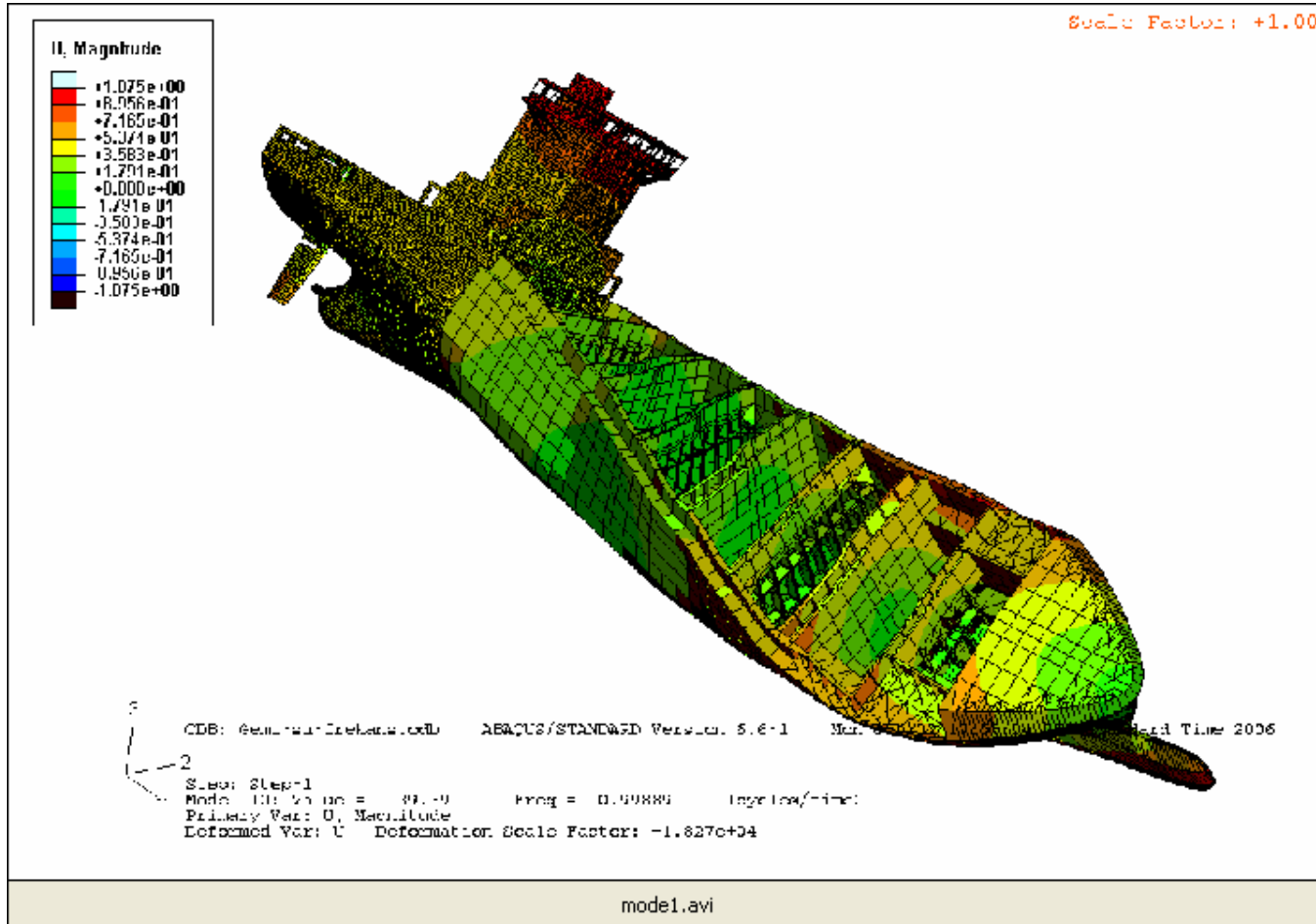




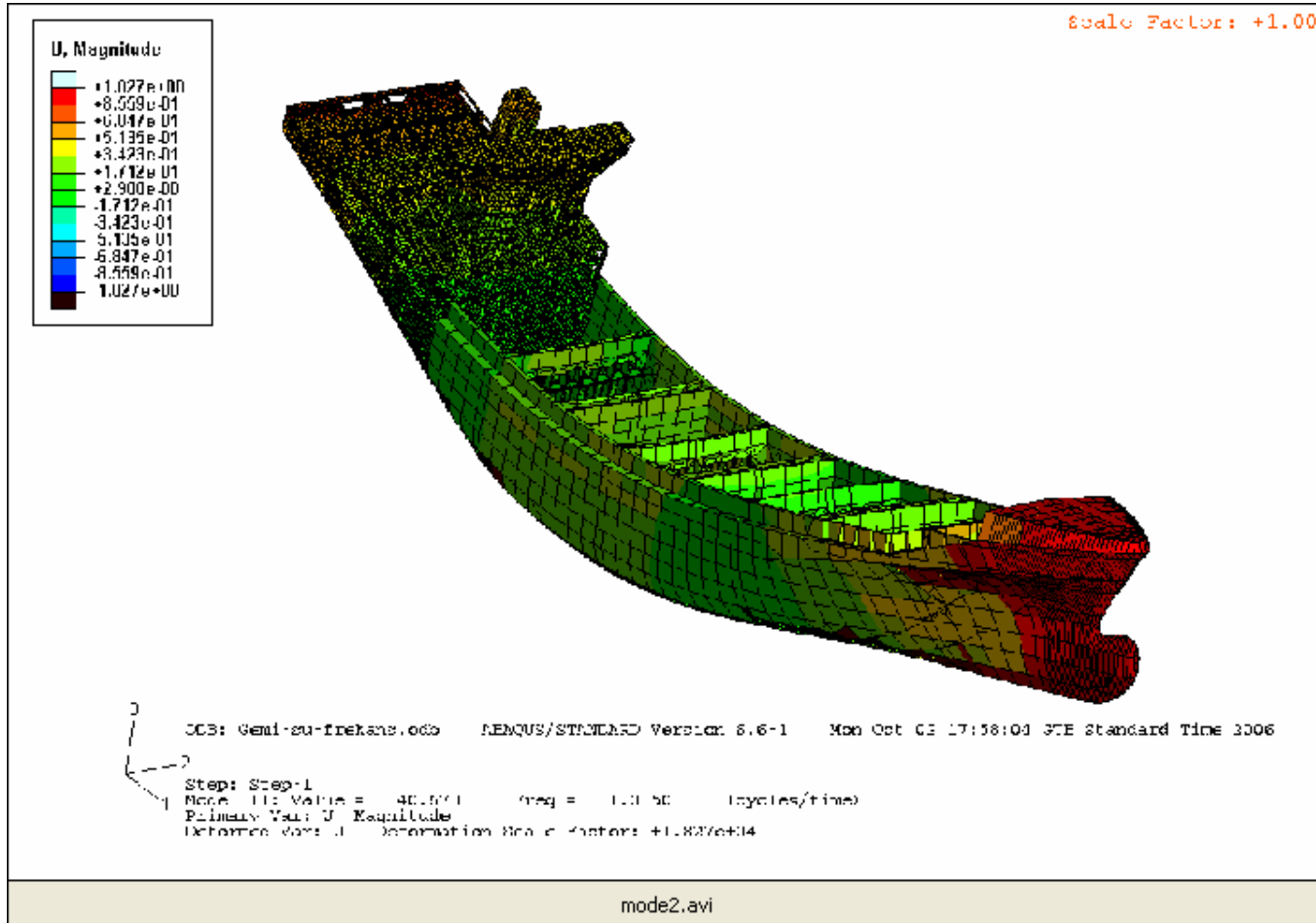




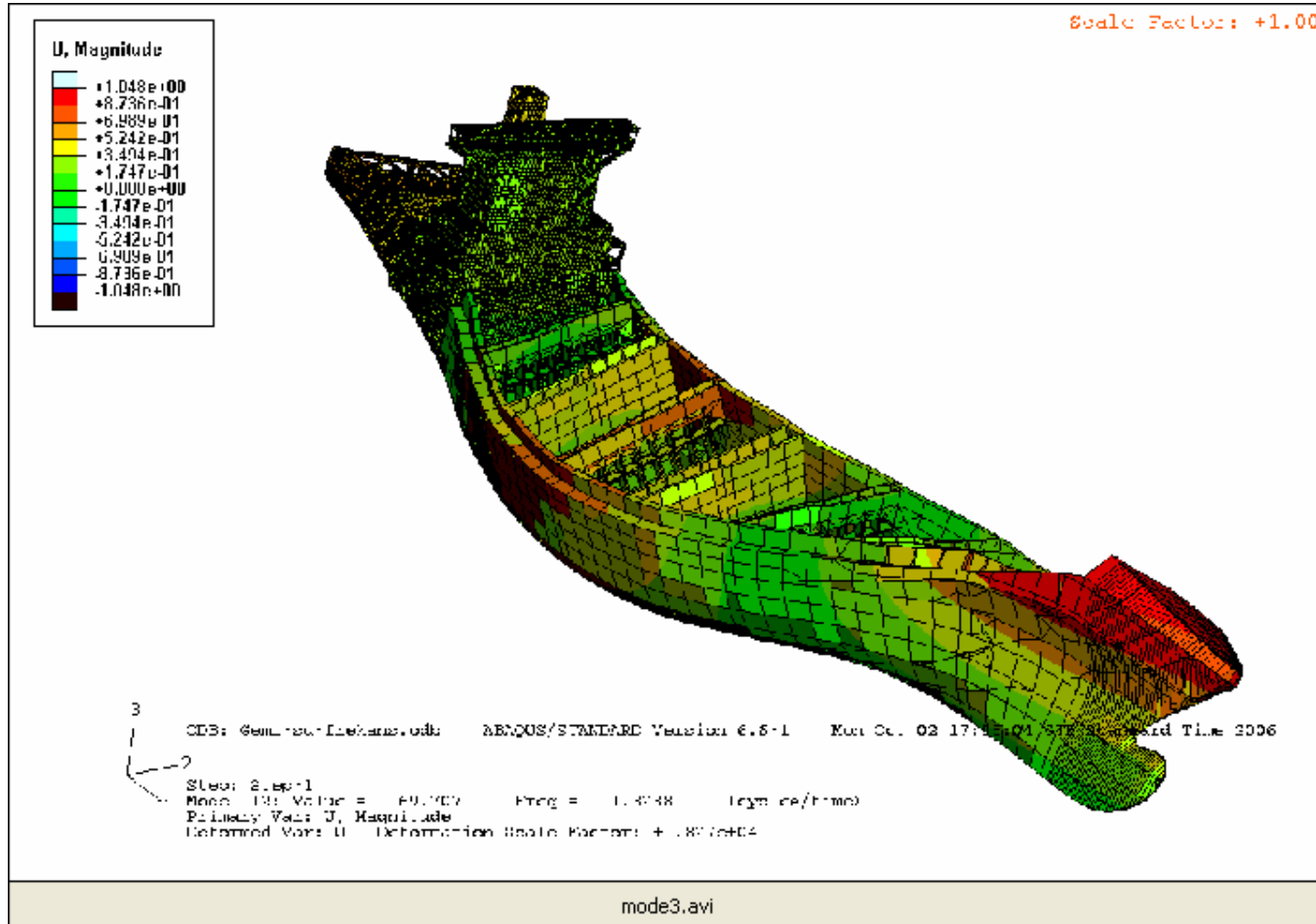
Dry Freq = 1.119 Hz



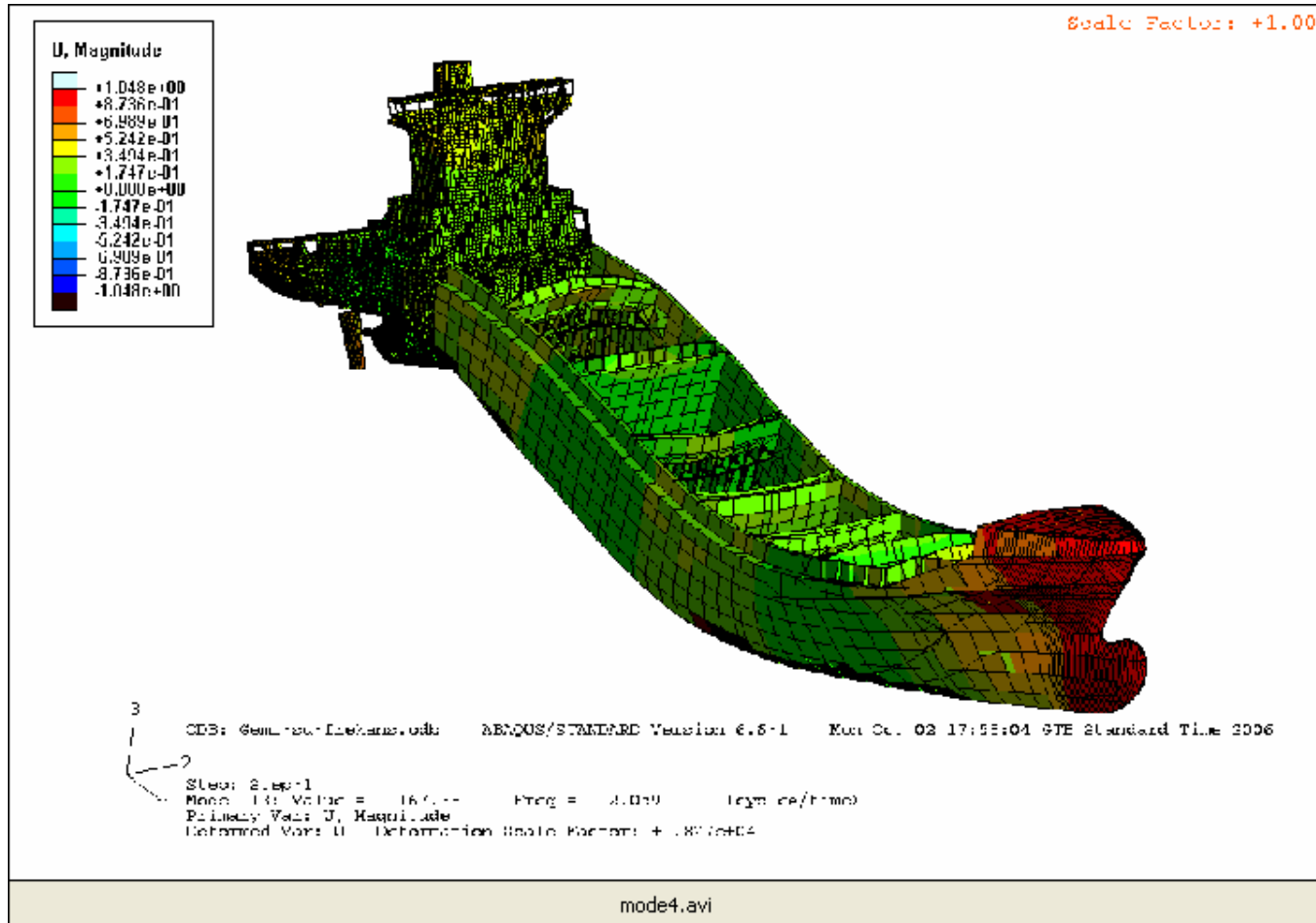
Dry Freq = 1.331 Hz



Dry Freq = 1.515 Hz

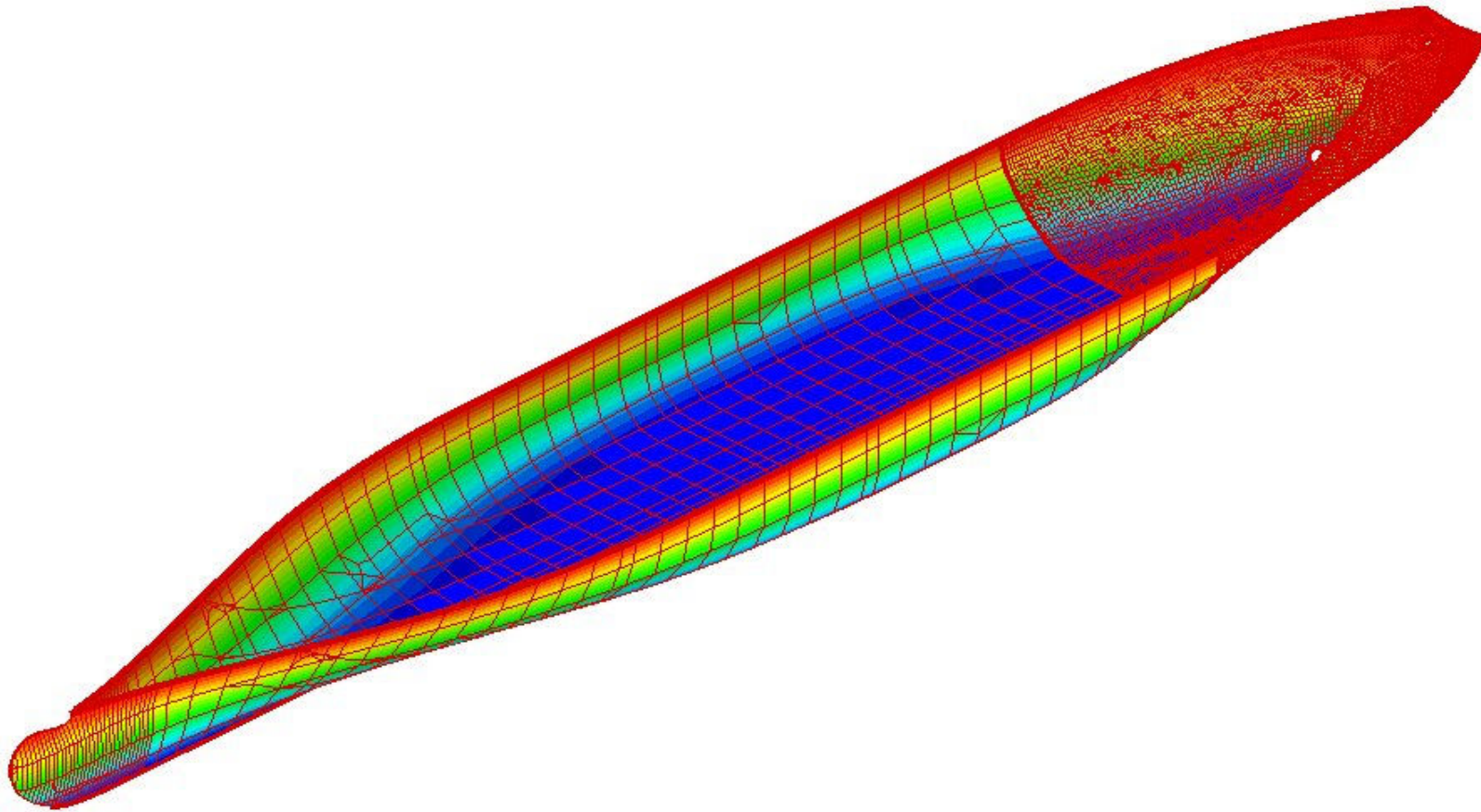


Dry Freq = 1.676 Hz



Hydroelastic Investigation of a 1900 TEU Container Ship – BE Model

- Number of nodes = 10674
 - Number of elements = 10772
- 12 in vacuo modes employed in the analysis



generalized added mass (kgm²)
 (1st ten modes, corresponding to 1 kgm² generalized structural mass)

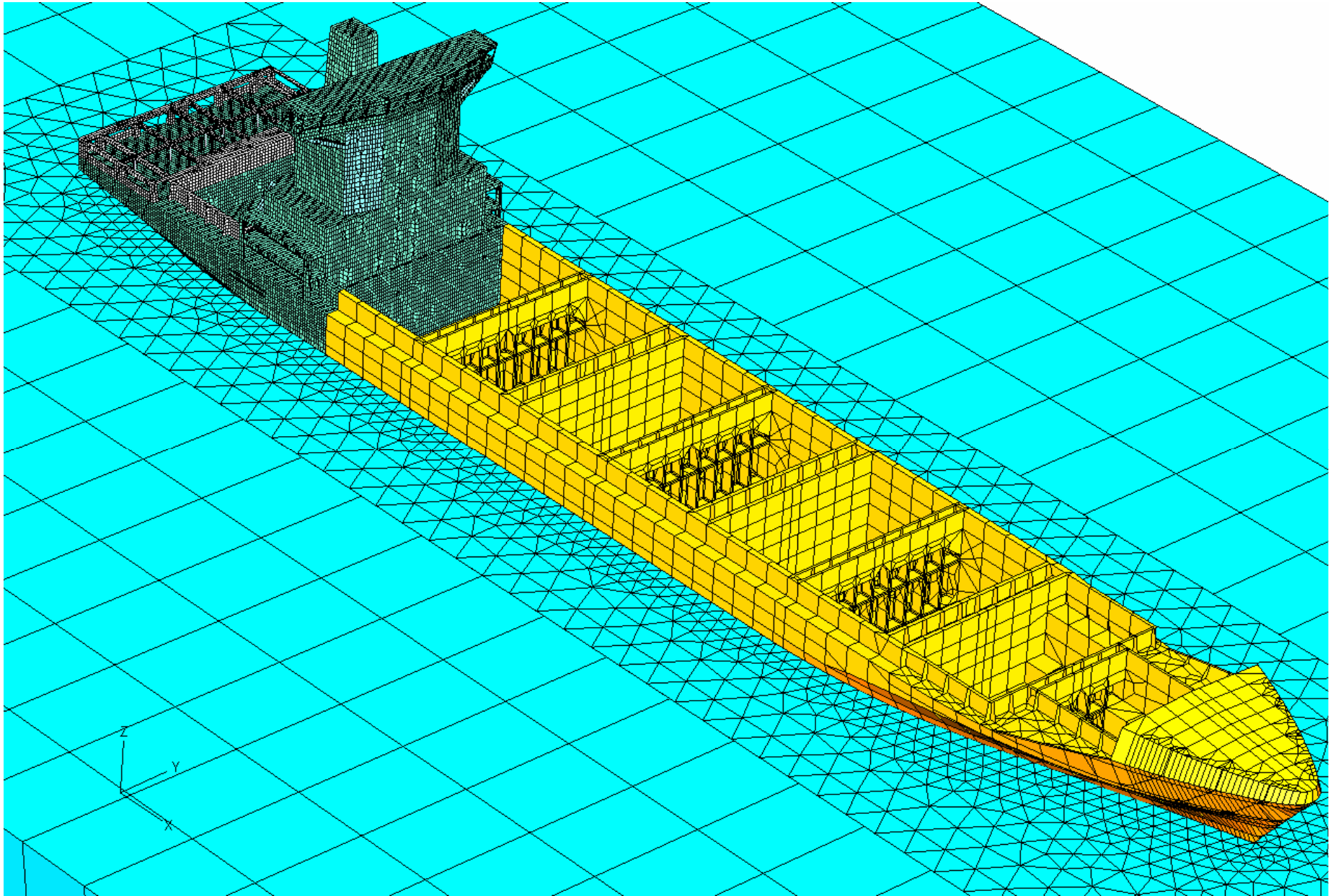
	1	2	3	4	5	6	7	8	9	10
1	0.24	0.00	0.11	0.03	0.00	-0.09	0.11	0.00	-0.01	0.00
2	0.00	0.63	0.00	0.00	-0.06	0.00	0.00	0.20	0.00	0.04
3	0.07	0.00	0.27	-0.02	0.00	0.00	0.08	0.00	0.01	0.00
4	0.03	0.00	-0.05	0.17	-0.01	0.03	-0.05	0.00	-0.02	0.00
5	0.00	-0.07	0.00	0.00	0.67	0.00	0.00	0.04	0.00	-0.01
6	-0.07	0.00	0.00	0.02	0.00	0.20	-0.08	0.00	0.02	0.00
7	0.45	0.00	0.50	-0.15	0.00	-0.38	0.58	0.00	-0.03	-0.02
8	0.00	0.32	0.00	0.00	0.05	0.00	0.00	0.49	0.00	-0.04
9	-0.01	0.00	0.01	-0.02	0.00	0.03	-0.01	0.00	0.15	0.00
10	-0.01	0.09	-0.01	0.00	-0.02	0.01	-0.01	-0.06	0.01	0.06

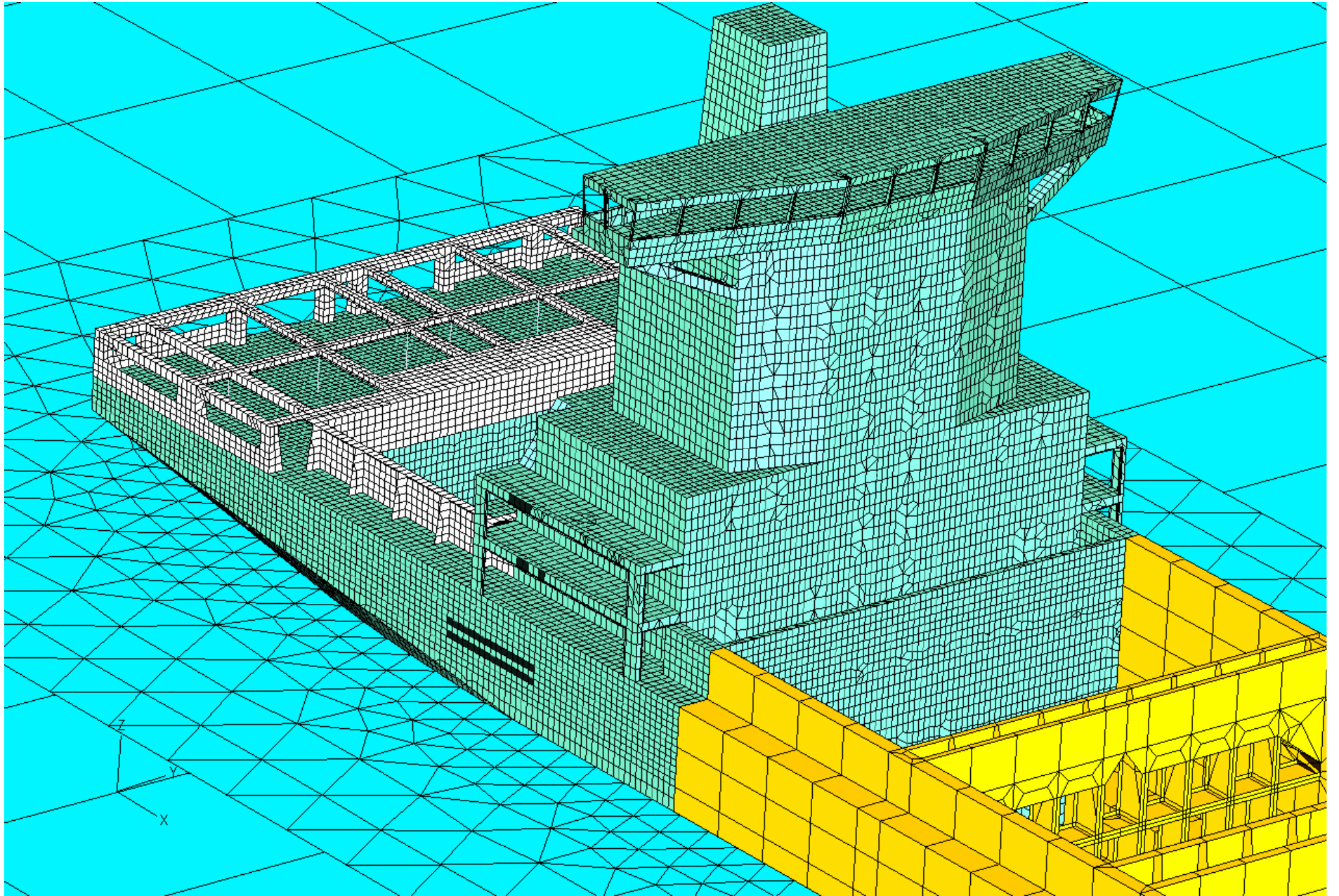
principle coordinates (1st ten modes)

	1	2	3	4	5	6	7	8	9	10
1	1.00	0.01	0.08	0.01	0.00	-0.01	0.04	0.00	0.00	0.00
2	0.01	-1.00	0.00	0.00	0.01	0.00	0.00	-0.03	0.00	-0.01
3	-0.21	0.00	0.98	-0.02	0.00	0.00	0.07	0.00	0.00	0.00
4	0.00	0.05	0.00	-0.02	1.00	0.00	0.00	0.03	0.00	-0.01
5	0.01	0.00	-0.04	-0.98	-0.01	-0.04	0.17	0.00	0.01	0.00
6	0.12	0.00	0.07	-0.15	0.00	0.36	-0.91	0.00	0.02	0.01
7	0.04	0.01	0.07	-0.05	0.00	-0.52	-0.84	-0.07	-0.01	0.01
8	0.00	0.13	-0.01	0.01	0.04	0.07	0.10	-0.96	0.01	0.07
9	0.01	0.00	-0.01	0.03	0.00	-0.04	0.03	0.01	1.00	0.02
10	0.00	0.02	0.00	0.00	-0.04	0.00	-0.01	0.02	0.01	-0.64

Hydroelastic Investigation of a 1900 TEU Container Ship – FE Wet Model

- 60300 fluid elements are used to model the behavior of fluid surrounding the ship hull.



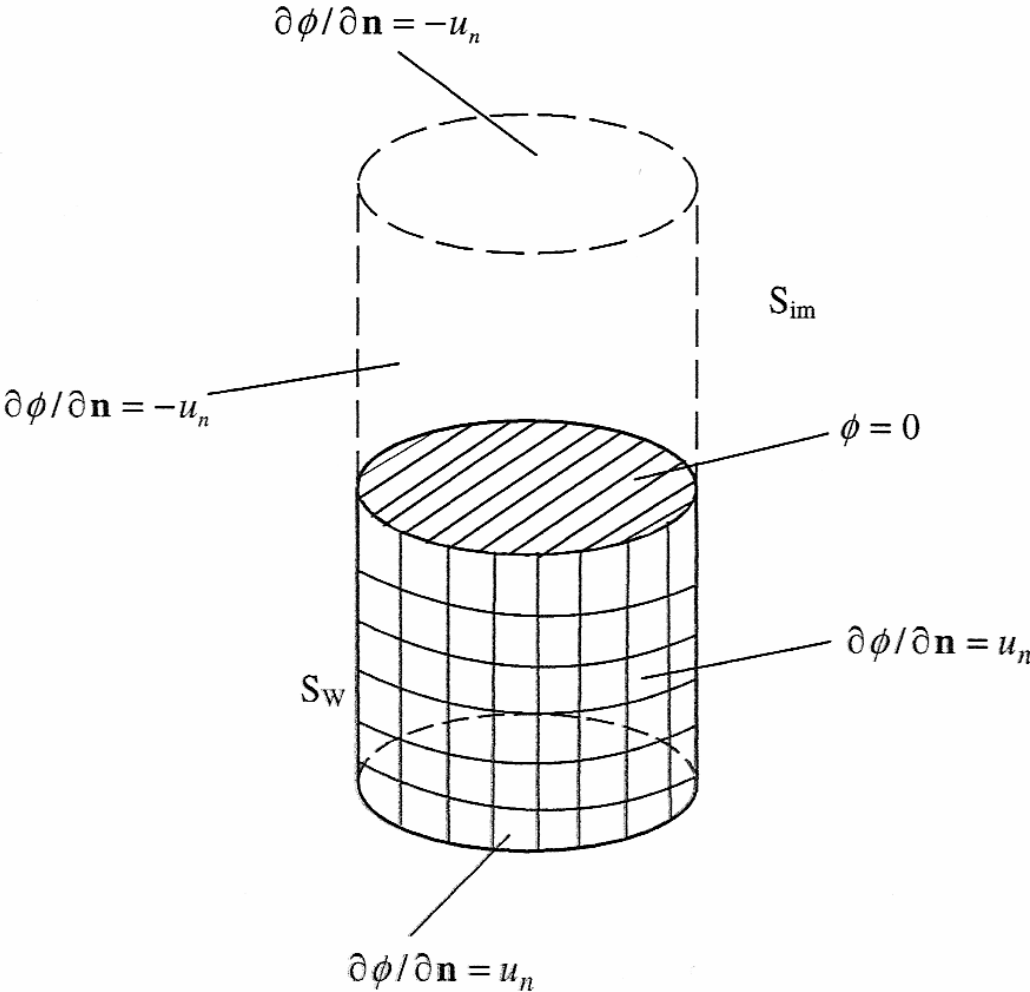


Comparison of Wet BE and FE Results

global vibration mode	dry	wet freq (Hz)		
	freq (Hz)	fem	bem	err
1st torsion	1.119	0.998	0.998	0.0
1st bending	1.331	1.015	1.041	2.5
1st hor. bending & tors.	1.515	1.328	1.348	1.5
2nd torsion	2.547	2.325	2.342	0.7
2nd bending	2.676	2.059	2.071	0.6

NUMERICAL RESULTS

Fluid Storage Tanks



NUMERICAL RESULTS

Fluid Storage Tanks

Table 3

Comparisons of *dry* and *wet* natural frequencies for clamped–free cylindrical shell (Hz)

Mode (m, n)	Dry analysis			Wet analysis								
	This study	FEA [5]	Experiment [5]	$d/L = 0.5$			$d/L = 0.7$			$d/L = 1$		
				This study	FEA [5]	Experiment [5]	This study	FEA [5]	Experiment [5]	This study	FEA [5]	Experiment [5]
1,3	634.2	633	616	608.9	609.4	542.0	543.1	522	400.7	400.6	388	
1,2	814.2	814	708	769.3	771.1	669.8	672.7	582	481.1	482.1	421	
1,4	949.2	947	945	908.4	908.8	806.8	806.0	798	635.3	633.2	628	
1,5	1482.5	1480	1479	1351.8	1352.8	1195.5	1188.4	1196	1039.7	1033.0	1027	
2,4	1649.8	1648	1628	1308.4	1303.9	1261.4	1253.2	1244	1111.8	1110.6	1094	
1,1	1825.6	1827	—	1654.7	1654.4	1407.3	1407.4	—	1041.9	1038.6	—	
2,5	1840.3	1839	1851	1571.3	1565.8	1557.7	1553.8	1546	1305.0	1304.2	1299	
2,3	2029.9	2029	1969	1519.9	1515.2	1434.0	1425.3	1394	1288.0	1286.9	1245	
1,6	2156.8	2154	2151	1843.5	1842.7	1693.6	1679.7	—	1574.3	1561.3	1546	
2,6	2385.8	—	—	2189.6	2189.0	2119.7	—	—	1762.4	1762.6	1748	

[5] T. Mazúch, J. Horáček, J. Trnka, J. Veselý, Natural modes and frequencies of a thin clamped-free cylindrical storage tank partially filled with water: FEM and measurements, *Journal of Sound and Vibration*, Vol.193, pp.669-690, 1996

NUMERICAL RESULTS

Fluid Storage Tanks

A. Ergin, B. Uğurlu / Journal of Sound and Vibration 275 (2004) 489–513

501

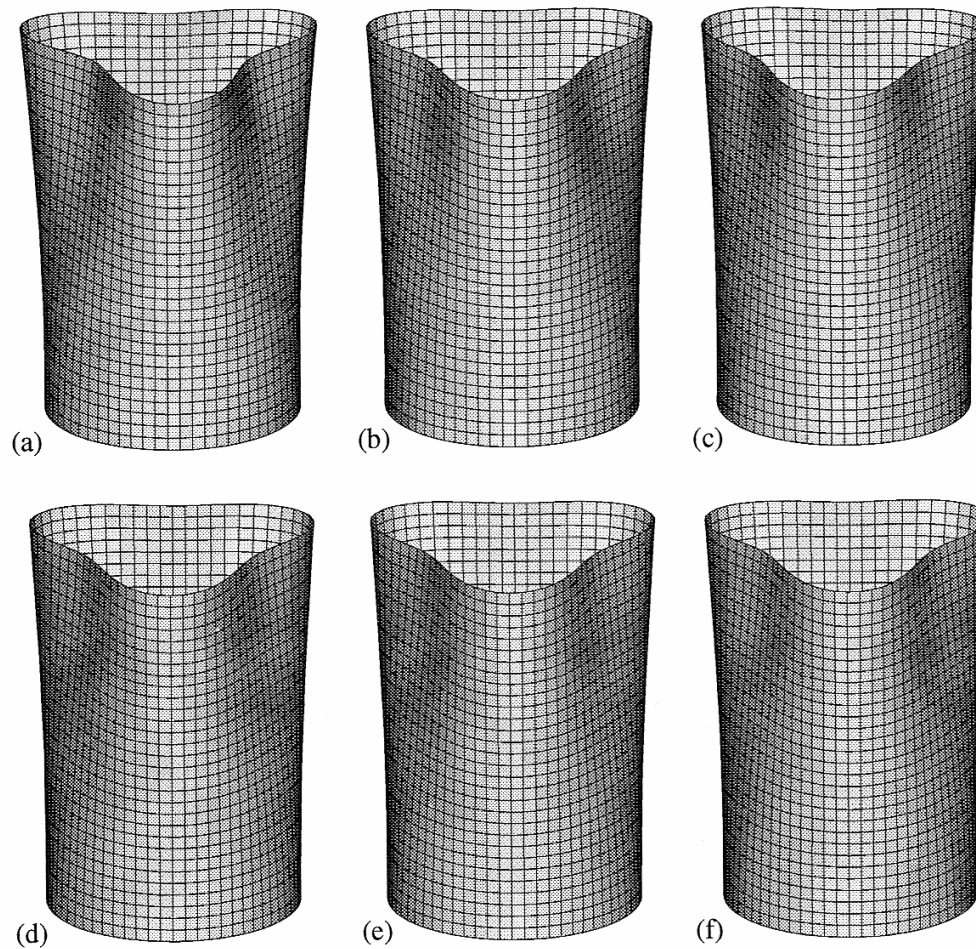


Fig. 4. Predicted mode shapes with $m = 1$ and $n = 3$: (a) empty shell, $d/L = 0$; (b) $d/L = 0.2$; (c) $d/L = 0.4$; (d) $d/L = 0.6$; (e) $d/L = 0.8$; (f) $d/L = 1$.

NUMERICAL RESULTS

Fluid Storage Tanks

502

A. Ergin, B. Uğurlu / Journal of Sound and Vibration 275 (2004) 489–513

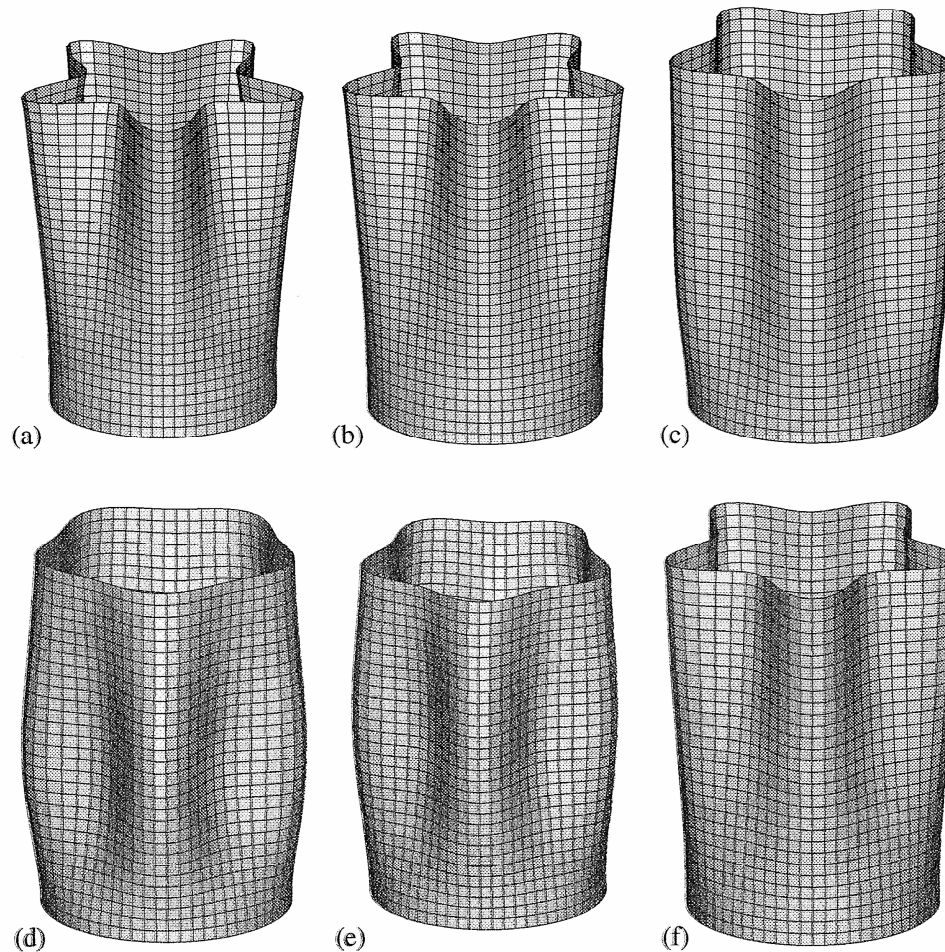


Fig. 5. Predicted mode shapes with $m = 1$ and $n = 5$: (a) empty shell, $d/L = 0$; (b) $d/L = 0.2$; (c) $d/L = 0.4$; (d) $d/L = 0.6$; (e) $d/L = 0.8$; (f) $d/L = 1$.

NUMERICAL RESULTS

Fluid Storage Tanks

A. Ergin, B. Uğurlu / Journal of Sound and Vibration 275 (2004) 489–513

511

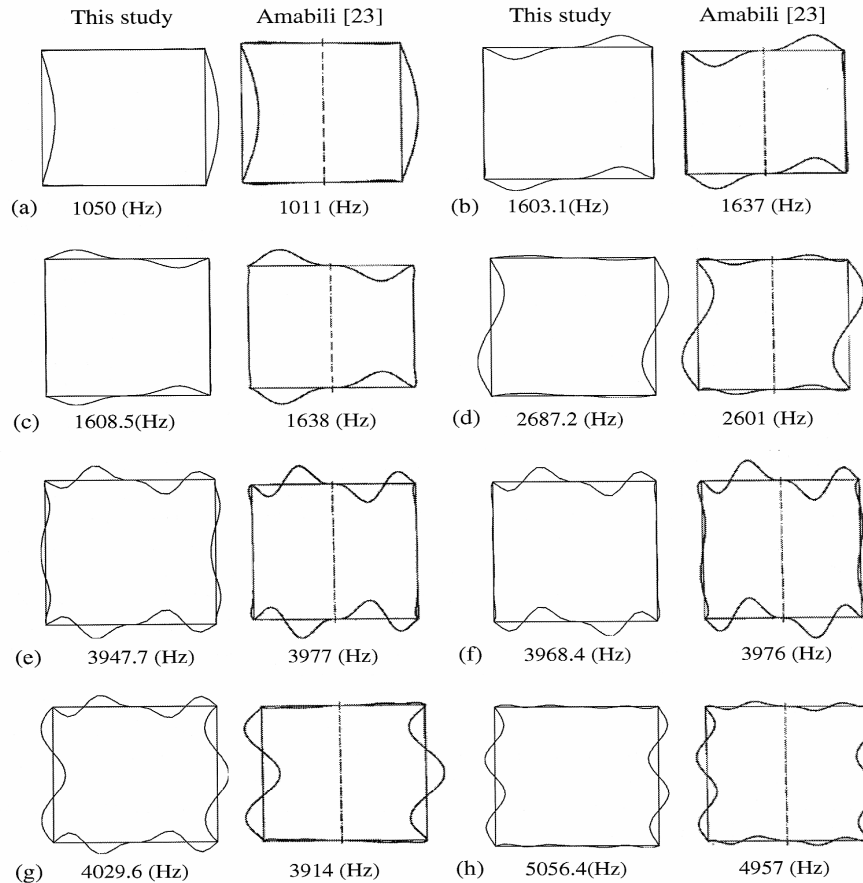


Fig. 7. Comparisons of predicted wet mode shapes of completely filled hermetic can for n (or i) = 3: (a) first symmetric shell-dominant mode; (b) first anti-symmetric plate-dominant mode; (c) first symmetric plate-dominant mode; (d) first anti-symmetric shell-dominant mode; (e) second symmetric plate-dominant mode; (f) second anti-symmetric plate-dominant mode; (g) second symmetric shell-dominant mode; (h) second anti-symmetric shell-dominant mode.

NUMERICAL RESULTS

Elastic Structure Containing Axial Flow

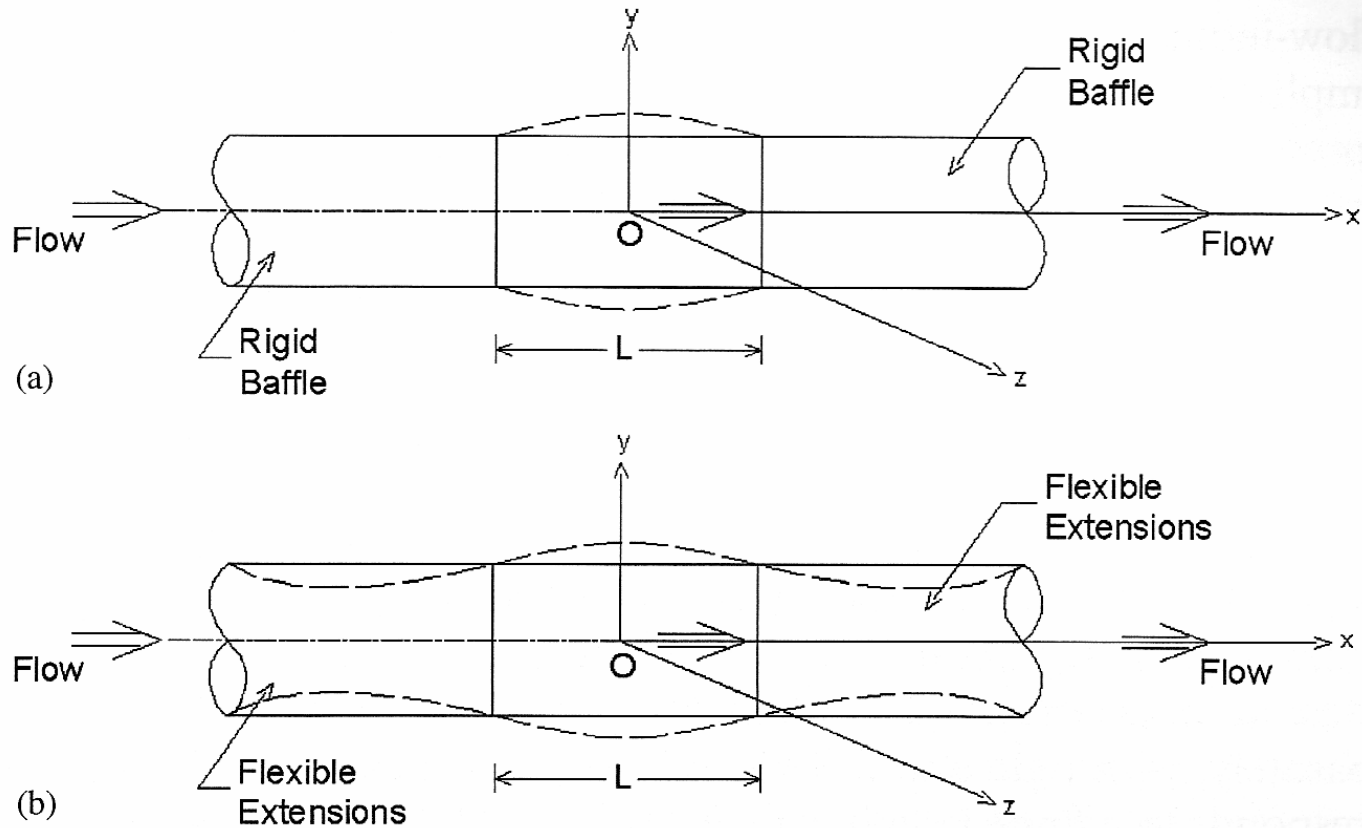


Fig. 1. Cylindrical shell conveying flowing fluid, (a) with rigid extensions and (b) with flexible extensions.

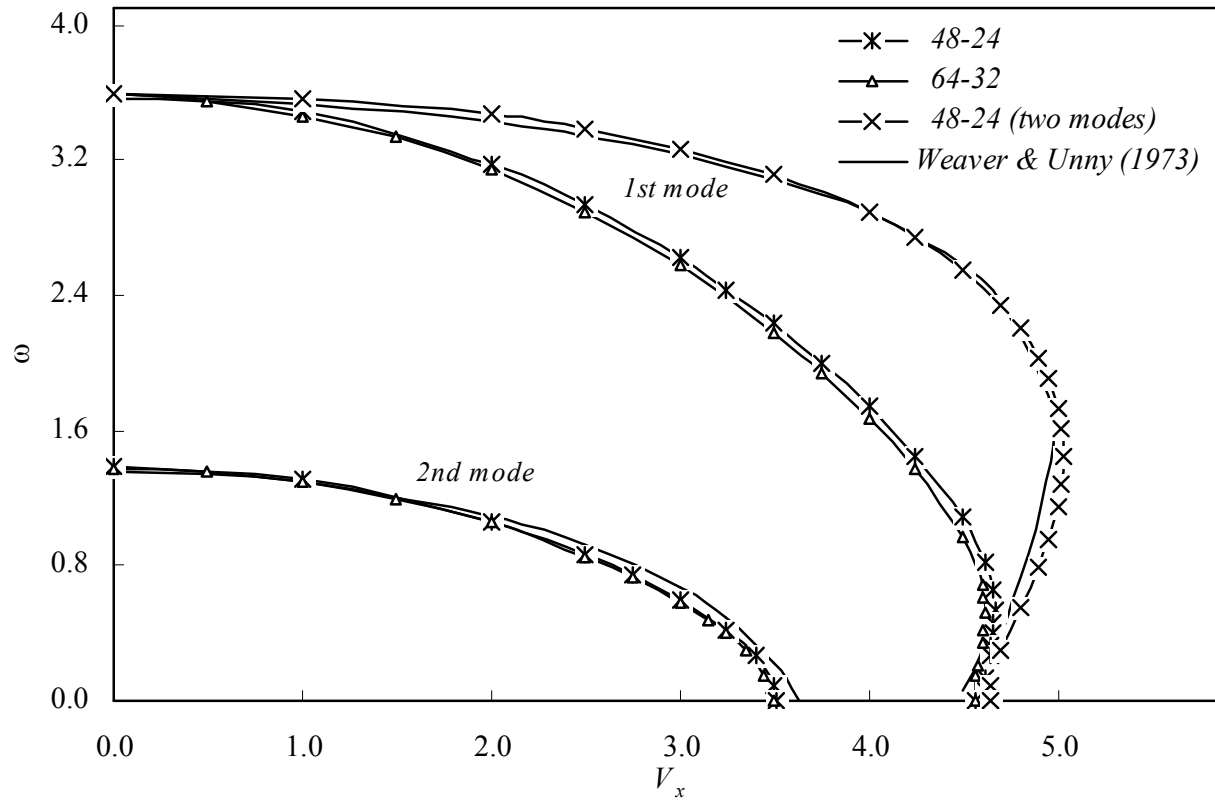
NUMERICAL RESULTS

Elastic Structure Containing Axial Flow

The structure adopted for calculations is a finite length cylindrical shell, simply supported at both ends, and it was analytically investigated by Weaver and Unny (1973), Selmane and Lakis (1997), Amabili *et al* (1999) and Amabili and Garziera (2002). The shell structure has the geometric and material properties: length-to-radius ratio $L/R = 2$, thickness-to-radius ratio $h/R = 0.01$, Young's modulus $E = 206$ GPa, Poisson's ratio $\nu = 0.3$, and mass density $\rho_s = 7850$ kg/m³. Fresh water is used as the contained fluid with a density of $\rho_f = 1000$ kg/m³.

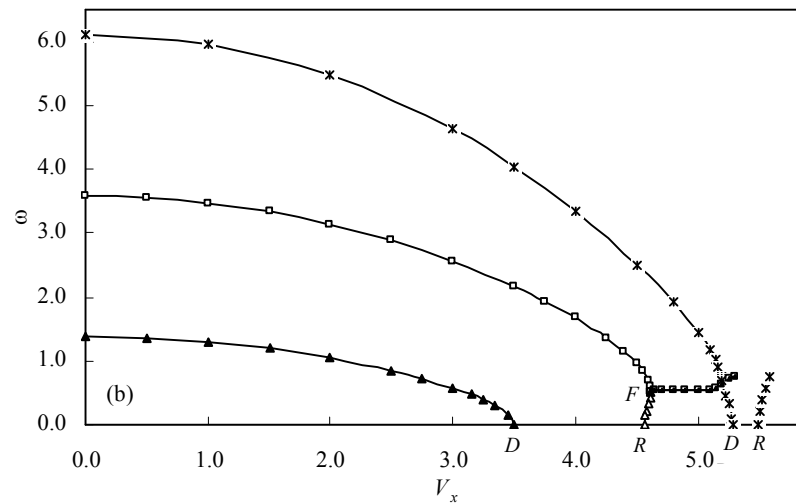
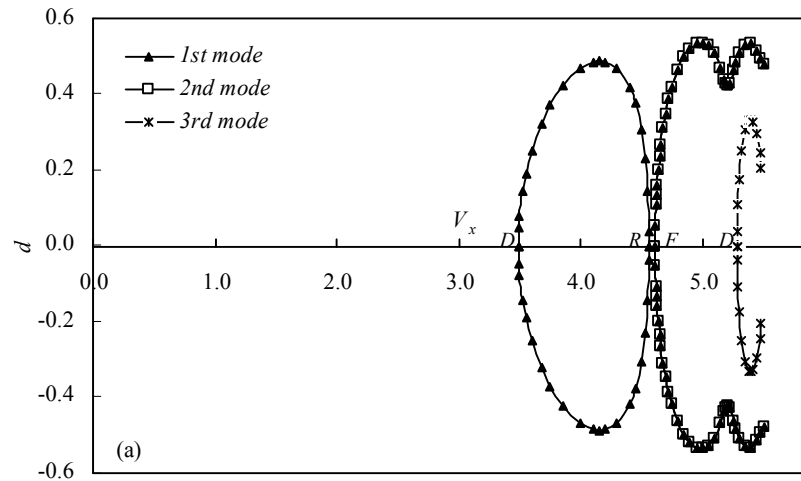
NUMERICAL RESULTS

Elastic Structure Containing Axial Flow



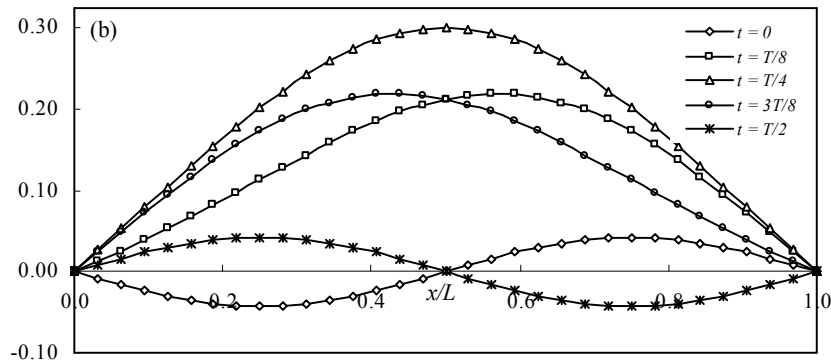
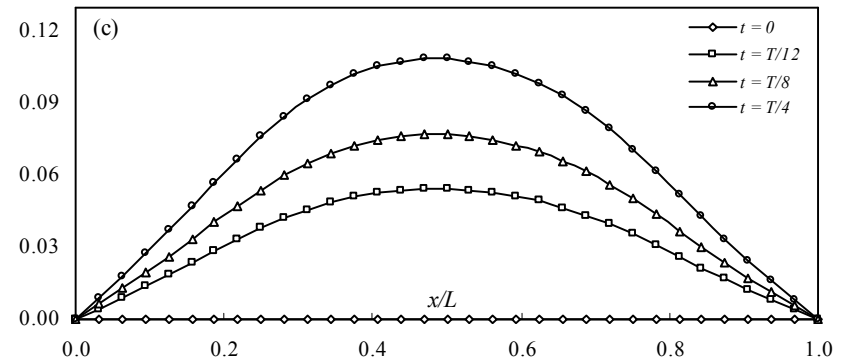
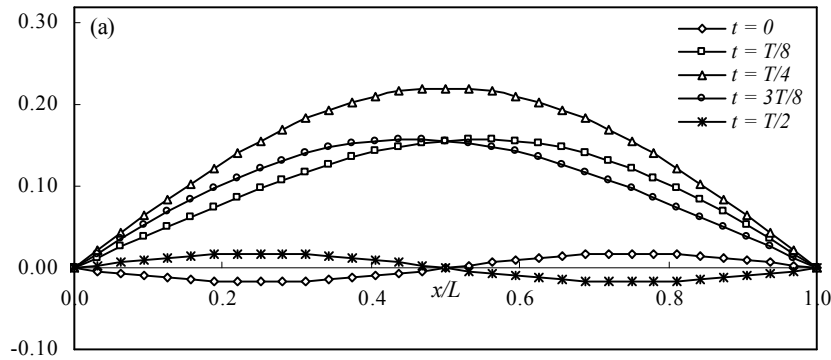
NUMERICAL RESULTS

Elastic Structure Containing Axial Flow



NUMERICAL RESULTS

Elastic Structure Containing Axial Flow



Conclusions

- It can also be said that the hybrid method introduced in this study can be applied to any shape of cylindrical structure partially in contact with internal and/or external flowing fluid, in contrast to the studies found in the literature.
- The present study has demonstrated the versatility of the method developed before and extended in this study further. By introducing the linearly varying boundary elements in this study, the convergence of the numerical predictions were obtained much faster than those using constant distributions over the boundary elements.
- the predicted frequency values behave as expected. It is to say that they decrease with increasing non-dimensional axial flow velocity, and they reach a zero frequency for the axial flow velocity at which a static divergence occurs.